APPENDIX A

A GENERAL MODEL OF COAL DEVOLATILIZATION

P.R. Solomon, D.G. Hamblen, R.M. Carangelo, M.A. Serio and G.V. Deshpande

Advanced Fuel Research, Inc., 87 Church St., East Hartford, CT 06108 USA

INTRODUCTION

Coal devolatilization is a process in which coal is transformed at elevated temperatures to produce gases, tar* and char. The combined chemical and physical processes in devolatilization have been reviewed by a number of investigators (1-6). Gas formation can often be related to the thermal decomposition of specific functional groups in the coal and can be predicted with reasonable accuracy simulated by models employing first order reactions with ultimate yields (5-16). On the other hand, tar and char formation are more complicated and success in mechanistic modeling of tar formation has been more limited.

Predicting tar formation is, however, important for several reasons. Tar is a major volatile product (up to 40% of the DAF coal weight for some bituminous coals). Tar yields vary substantially depending on reactor conditions (pressure, heating rate, final temperature, bed geometry, particle size, etc.). In combustion or gasification, tar is often the volatile product of highest initial yield and thus controls ignition and flame stability. It is a precursor to soot which is important to radiative heat transfer. The process of tar formation is linked to the char viscosity (16-19) and the subsequent physical and chemical structure of

*Tar is defined as the room temperature condensibles formed during coal devolatilization.

the char and so is important to char swelling and reactivity. Also, because tar molecules are sometimes minimally disturbed coal molecular fragments, primary tars provide important clues to the structure of the parent coal (5,6,20).

It is generally agreed that the tar formation includes the following steps: 1) depolymerization by rupture of weaker bridges in the coal macromolecule to release smaller fragments called metaplasts (3,5,7,16,21-33); 2) repolymerization (crosslinking) of metaplast molecules (3,5,7,16,21-33); 3) transport of lighter molecules away from the surface of the coal particles by combined vaporization and diffusion (23,32); 4) internal transport of lighter molecules to the surface of the coal particles by convection and diffusion in the pores of non-softening coals (24,27,34,35) and liquid phase or bubble transport in softening coals (17,36,37). Char is formed from the unreleased or recondensed fragments. Varying amounts of loosely bound "guest" molecules, usually associated with the extractable material, are also released in devolatilization.

The complexity of proposed devolatilization models varies substantially. They can be divided into four categories. The simplest are the "Weight Loss Models" employing a single rate (6,22,38-42), two rates (38,43), multiple parallel rates or distributed rates (9,22). These models do not account for the variations in tar yield with reaction conditions and a number of "Tar Formation Models" incorporating retrogressive char forming reactions and mass transport have been proposed which account for such variations (7,16,21-33,44-47).

Most of the above models do not consider the evolution of gas species, which have been treated in a number of "Species Evolution/Functional Group Models" as parallel first order reactions (5-13). More complicated "Comprehensive Chemical Models" also describe the composition of the char and tar (3,5,6,11-13,48,49).

The level of detail required in a model depends on its application. In modeling combustion and gasification the simple "Weight Loss Models" have often been employed. However, to predict the variations in yield with reactor conditions, the more complicated "Tar Formation Models" must be used. A case can also be made for employing the more complicated "Species Evolution/Functional Group Models" or "Comprehensive Chemical Models". For example, in predicting the energy released from combustion of the volatiles it is important to know that for low rank coals a high percentage of the volatiles may be non-combustible H_2O and CO_2. For a North Dakota lignite, the total of these two components can be as high as 35% of the rapidly released volatiles which are important for ignition (6). In addition, the swelling, particle agglomeration properties, char reactivity, and fragmentation are functions of the char composition. Soot formation (which can dominate radiative energy transport) is controlled by the tar amount.

In modeling liquefaction and mild gasification, knowledge of the chemical makeup and molecular weight distribution of the soluble and volatile products is essential, requiring the more complete "Comprehensive Chemical Models".

This paper presents a general mechanistic model for coal devolatilization which considers the evolution of gas, tar, char and guest molecules. Two previously developed models, a Functional Group (FG) model (5,6,11-13) (a "Species Evolution/Functional Group Model") and a Devolatilization-Vaporization-Crosslinking (DVC) model (30,31,44-47) (a "Tar Formation Model") are combined in a general FG-DVC model (a "Comprehensive Chemical Model").

The FG model considers the parallel independent evolution of the light gas species formed by the decomposition of functional groups. Alternatively, functional groups can be released from the coal molecule attached to molecular

fragments which evolve as tar. The kinetic rates for the decomposition of each functional group ard for tar formation have been determined by comparison to a wide variety of data (5,6,11-13). To a first approximation, these rates are insensitive to coal rank (5,6,49,50-53). The FG model used an adjustable parameter to fit the total amount of tar evolution. This parameter depends strongly on the details of the time-temperature history of the sample, the external pressure, and the coal concentration and, therefore, varies with the type of experiment performed.

The variation in tar yield with the above mentioned parameters can be predicted by the DVC model (30,31,44-47). In the DVC model, tar formation is viewed as a combined depolymerization and transport process in which the pyrolytic depolymerization continually reduces the weight of the coal molecular fragments through bond breaking and stabilization of free radicals, until the fragments are small enough to be transported out of the particle. This process continues until the donatable hydrogens are consumed. Simultaneously, crosslinking can occur. The model employs a Monte Carlo technique to perform a computer simulation of the combined depolymerization, crosslinking and transport events.

The original model considered transport away from the surface by vaporization and diffusion. Internal mass transport limitations were not included. However, current research (33) shows that considering the transport limitations of surface evaporation and film diffusion alone are not sufficient to predict the reduced tar yields when devolatilization occurs at low temperatures. An empirical expression for internal transport has, therefore, been added to the DVC model (33).

These two models have been combined as subroutines of the general FG-DVC model to eliminate their respective deficiencies (33). The DVC subroutine is employed to determine the yield of tar and the molecular weight distribution of the tar and

char. The FG subroutine is used to describe the gas evolution, and the elemental and functional group compositions of the tar and char. The crosslinking is predicted by assuming that this event can be correlated with gas evolution.

The FG-DVC model is general in its applicability to bituminous coals, subbituminous coals and lignites (employing rank independent kinetic parameters), in its application to reactors of widely differing heating rates (0.05°C/sec to 20,000°C/sec) and in its ability to predict the variations in tar yield with reactor conditions.

The FG-DVC model is mechanistic in its use of separate rate equations to describe each observed chemical or physical reaction in devolatilization. For example, gas evolution is coupled to the changing composition of its functional group source in the parent coal, with a separate equation to describe each functional group. The model does not attempt to describe the detailed chemistry of each reaction, but instead uses global rates. The FG-DVC model is thus intermediate between a completely mechanistic model which would describe the chemical reactions in detail (a good framework is, however, provided for such models) and a purely empirical model which attempts to minimize the number of rate equations, but in which the rate equations may not necessarily be related to observable processes.

The model describes the processes of:

1) **Depolymerization and Hydrogen Consumption**
2) **Crosslinking**
3) **External Transport**
4) **Internal Transport**

5) **Gas Formation for all principal species**

6) **Tar Composition**

7) **Char Composition**

Because the FG-DVC model predicts all the principal gas species, it requires a large number of rates, composition parameters, and equations. However, a substantial reduction in the numerical parameters required is made by the use of rank independent kinetic parameters. These parameters have already been determined using a wide variety of coals and reactors. This simplification appears to be a good first approximation to describe the kinetics of individual evolved species or functional group decompositions (5,6,50-53). The composition parameters also vary systematically with coal elemental composition.

In addition, if chemical detail in the prediction is not required, the gas equations can be lumped into a single equation with one rate and one composition parameter to simplify the model. In that case, only five equations (depolymerization, crosslinking, external transport, internal transport, and gas formation) and four kinetic rates (one bond breaking rate, two crosslinking rates, and one gas formation rate) are required for the reduced FG-DVC model.

The paper describes the two models and how they have been combined. The work presented here is limited to dilute phase reactions of small coal particles where internal temperature gradients can be neglected. Secondary gas phase reactions have been discussed elsewhere (6) and reactions of pyrolysis products with a char bed and large particle effects have not yet been included. Only reactions involving C, H, and O are discussed here. The coal composition and reactor conditions (pressure, particle time-temperature history) are required to predict the pyrolysis behavior.

The properties predicted as a function of time, include: **TAR** - molecular weight distribution, elemental and functional group composition, yield; **CHAR** - molecular weight distribution, elemental and functional group composition, yield, crosslink density, extract yield, viscosity; **GAS** - yields of individual light gas species. Results are presented for a Pittsburgh Seam bituminous coal and a North Dakota lignite.

EXPERIMENTAL

COALS EXAMINED

The two coals described in this paper are a Pittsburgh Seam bituminous coal and a North Dakota (Beulah) lignite. Samples of the Pittsburgh Seam coal were obtained from the Pittsburgh Energy Technology Center and the Argonne National Laboratory premium coal sample collection. Samples of the North Dakota (Beulah) lignite were obtained from the University of North Dakota Energy Research Center and the Argonne National Laboratory premium coal sample collection. Data on the premium samples are presented in Ref. 54 and on the other two samples in Ref. 6. The FG-DVC model was also compared to data on Pittsburgh coal samples from Refs. 7,16 and 22, and characterization of these samples are presented therein.

COAL CHARACTERIZATION

The crosslink density was estimated using the volumetric swelling technique developed by Larsen and co-workers (55-57). Pyridine extract yields were obtained using a Soxhlet apparatus. Molecular weight distributions of tars were obtained at SRI International using the Field Ionization Mass Spectrometry (FIMS) apparatus described by St. John et al. (58). Tar samples were collected from the pyrolysis apparatus and vaporized from a heated probe into the FIMS apparatus. In addition, coal samples were pyrolyzed directly in the FIMS apparatus.

APPARATUS

Pyrolysis experiments were performed in several apparatuses which have been described previously including: a heated grid pyrolyzer (5,12), a heated tube

reactor (6,13), and a thermogravimetric analyzer with analysis of evolved products by Fourier Transform Infrared (FT-IR) Spectroscopy (TG-FTIR) (6,59).

GENERAL MODEL

DESCRIPTION OF COAL DEVOLATILIZATION

Any general model of a process as complicated as coal devolatilization must of course be a gross approximation. However, there are many general trends which have been observed in devolatilization. The trick in developing a model is to pick a set of first approximations which best match the majority of these trends. There will of course be exceptions to the trends. These exceptions can be treated as perturbations to the first order approximation. Differences in models result because of the subjective choice of what is a general trend and what is an exception. The following discussion presents the authors' view of the general trends and the exceptions.

The General Trends

The general model of coal pyrolysis is based on a number of observations which have been previously made concerning coal pyrolysis. These are: i) pyrolysis species kinetics are insensitive to rank (5,6,11-13,50-53); ii) species amounts vary with coal rank and can be correlated with the coal's functional groups composition (5,6,14,15,48-50). The evolution of each species can be correlated with the change in the corresponding functional group composition in the char (5,6,50); iii) the primary tar composition is similar (except for a higher concentration of methyl groups) to that of the parent coal for bituminous coals and rapidly heated low rank coal (5,20,45,60-62); iv) tar yields are controlled by the amount of donatable hydrogen and how efficiently it is used (5,6,20,46); and v) crosslinking correlates with CO_2 and CH_4 evolution (63).

The general outline of devolatilization based on these observations was presented by Solomon and Hamblen (5) and Serio et al. (6). Fig. 1 from Ref. 6 presents a hypothetical picture of the coal's or char's organic structure at successive stages of devolatilization. The figure represents: a) the raw coal, b) the formation of tar and light hydrocarbons during primary pyrolysis, and c) char condensation and crosslinking during secondary pyrolysis. The hypothetical structure in Fig. 1a represents the chemical and functional group compositions for a Pittsburgh Seam bituminous coal as discussed by Solomon (20). It consists of aromatic and hydroaromatic clusters linked by aliphatic bridges. During pyrolysis, the weakest bridges, labeled 1 and 2 in Fig. 1a, can break producing molecular fragments (depolymerization). The fragments abstract hydrogen from the hydroaromatics or aliphatics, thus increasing the aromatic hydrogen concentration. These fragments will be released as tar if they can get to a surface and if they are small enough to vaporize under typical pyrolysis conditions (assuming the vaporization law proposed by Suuberg et al. (32)). The two lightest fragments are labeled tar. The other two fragments are shown to have repolymerized, producing a molecule which is too large to vaporize.

The other events during primary pyrolysis are the decomposition of functional groups to release CO_2, light aliphatic gases and some CH_4 and H_2O. The release of CH_4, CO_2, and H_2O may produce crosslinking, CH_4 by a substitution reaction in which the attachment of a larger molecule releases the methyl group, CO_2 by condensation after a radical is formed on the ring when a carboxyl is removed and H_2O by the condensation of two OH groups to produce an ether link (labeled 3 in Fig. 1b). The crosslinking is important to determine the release of tar and the visco-elastic properties of the char.

The end of primary pyrolysis occurs when the donatable hydrogen from

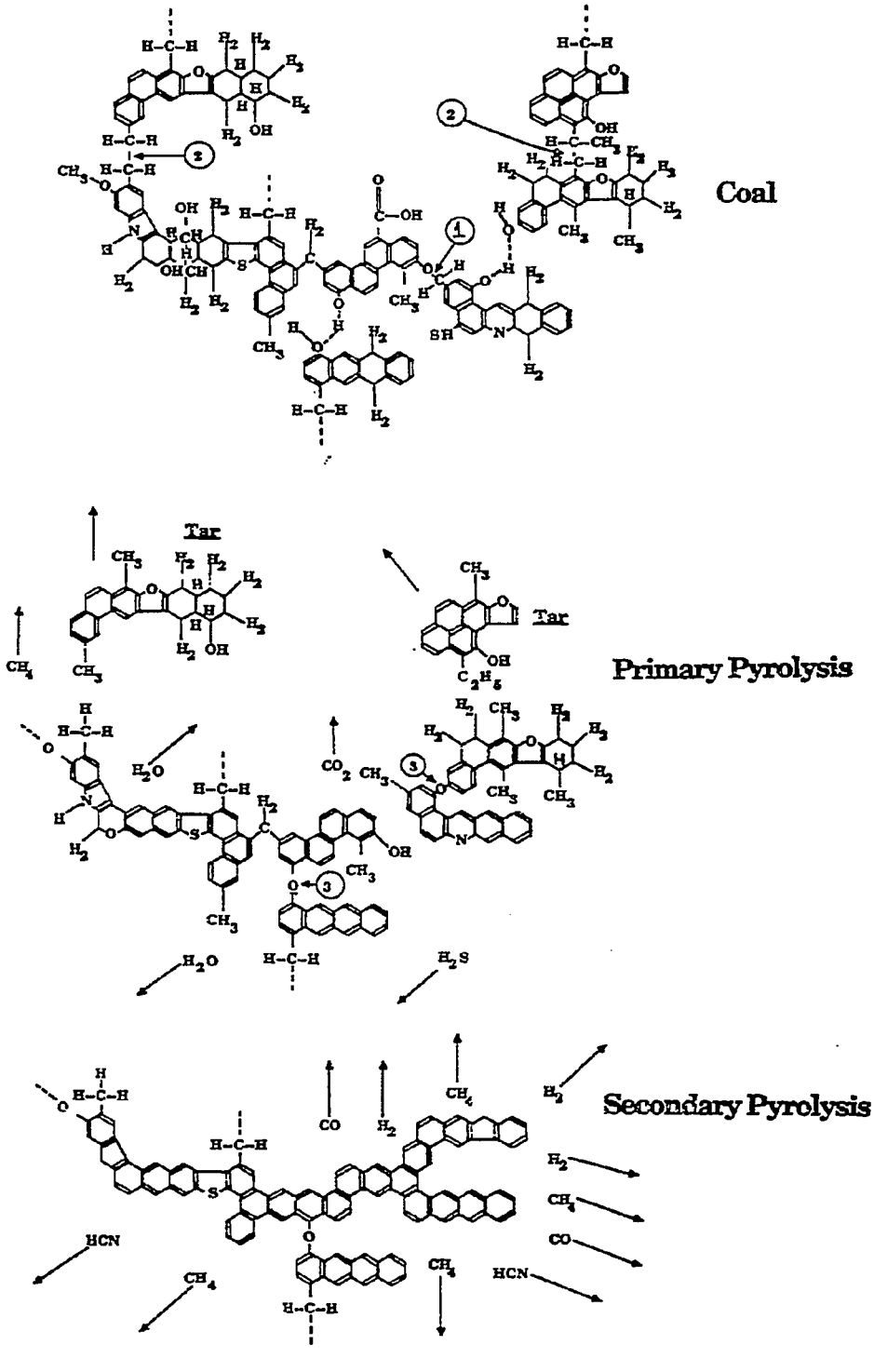

Figure 1. Hypothetical Coal Molecule During Stages of Pyrolysis. (Reprinted from Reference 6 with permission).

hydroaromatics or aliphatics is depleted. During secondary pyrolysis (Fig. 1c) there is additional methane evolution (from methyl groups), HCN from ring nitrogen compounds, CO from ether links, and H_2 from ring condensation. These general concepts are incorporated into the combined FG-DVC model as described below.

The Exceptions

Polymethylene - The major exception to the trends described above is the presence of varying amounts (typically 0 to 9%, but in some cases as high as 18%) of long chain aliphatics (polymethylenes). These have recently been reported in pyrolysis products by Nelson (64), by Calkins and co-workers (65-68), and references quoted therein. The chains appear alone and attached to aromatic nucleii (64). During devolatilization, the smaller molecules may be released without bond breaking and the heavier molecules with bond breaking to contribute to the tar. The presence of these polymethylenes make the tar more aliphatic than the parent coal. Further cracking of this material under more severe devolatilization conditions produces ethylene, propylene and butadiene from which the concentration of polymethylenes may be determined (67). The polymethylenes are included in the FG model as part of the aliphatic functional group which is assumed to decompose to produce gas products, not tar. If the amount of heavy polymethylenes is determined, these can be computed as a separate functional group with an appropriate release rate and added to the tar. The modeling of polymethylene evolution will be the subject of a subsequent publication.

Tar/Coal Similarities - The general model assumed as a first approximation that tar is derived from material of the same average composition as that of the parent coal. The model predicts that the tar is richer than the parent coal in methyl groups (due to hydrogen stabilization) and poorer in the rapidly removed

functional groups. Evidence for this assumption is the similarity in elemental compositions, infrared spectra and NMR spectra (5,20,45,60-62) observed for bituminous coals. It was, however, noted (5,45,69) that the infrared spectrum for a lignite tar was significantly different from that of the parent coal. The tar is much richer in aliphatic groups and poorer in oxygen functional groups. Freihaut et al. have recently reported a systematic increase in the tar hydrogen concentration with decreasing rank which suggests a similar trend (70).

There are at least two reasons for this variation with rank. One reason is the influence of the polymethylene groups. As noted by Calkins (67), the concentration of polymethylenes increases with decreasing rank (~4% for high volatile bituminous compare to ~8% for lignites). In addition, the tar yield decreases with decreasing rank, (~6% for the North Dakota lignite compared to 30% for the Pittsburgh Seam bituminous coal). The relative contribution of the polymethylenes to the tar is therefore increased with decreasing rank. This will lead to a higher aliphatic content and lower oxygen content for the low rank coal tar. This effect can be treated in the FG-DVC model by the addition of polymethylenes to the tar. A second reason is that the extensive crosslinking in low rank coals is related to the carboxyl group concentration which increases with decreasing rank. This crosslinking will thus selectively repolymerize the fragments rich in oxygen while those poorer in oxygen are more likely to be released as tar. This effect has not as yet been included in the model.

It is interesting to note an exception to the above observations. At very high heating rates, the North Dakota (Beulah) lignite is observed to melt and swell and produce a higher yield of tar which resembles the parent coal (13,30,31). The high heating rate appears to reduce the effect of crosslinking, leading to higher oxygen concentrations in the tar and to increased yields. Both effects enhance the

resemblance to the parent coal.

Variations of Kinetic Rates with Rank - While the model assumes rank independent kinetic rates, there is a systematic variation of rate with rank. As reported by Solomon and Hamblen (50), the variation between a lignite and bituminous coal results in a 50-75°C difference in the peak evolution temperature for most species. Systematic rank variations in the rate constants can be added to the model if increased accuracy is desired.

Macerals - Individual macerals are not considered in this model. The influence of the maceral concentration is assumed to occur through its effect on the average elemental and functional group composition. If details on macerals are desired then each maceral must be treated as a distinct molecular population with its own functional group composition and molecular weight distribution.

Physical Properties of Molecular Fragments - The general model has assumed that the vaporization and solubility of the molecular fragments are functions of molecular weight alone. Both properties are expected to depend on functional group composition. Such effects can be included as corrections to the vaporization law and solubility assumptions.

FORMULATION OF THE COMBINED FG-DVC MODEL

A detailed description of the pyrolysis behavior of coal is obtained by combining the previously developed DVC and FG models as subroutines in one general model. The FG subroutine, predicts the gas yields, and using the correlation developed for crosslinking with gas yields, it also determines the rate and number of crosslinks formed for the DVC subroutine, assuming one crosslink is formed per

CO_2 or CH_4 molecule evolved. The DVC subroutine supplies the tar yield to the FG subroutine, replacing what was previously an adjustable parameter. It also supplies the number of new methyl groups formed and the concentration of labile and unbreakable bridges. The two models are outlined below.

The Depolymerization-Vaporization-Crosslinking (DVC) Model Formulation

The DVC model has been described in a number of publications (30,31,44-47). It predicts the tar yield, the tar molecular weight distribution, the char yield, the char molecular weight distribution, the extract yield and the crosslink density. The model had its beginning in a study of polymers representative of structural features found in coal (44). The objective of that study was to develop an understanding of coal pyrolysis by studying a simpler, more easily interpretable system. The polymers were studied in a series of pyrolysis experiments in which tar amounts and molecular weights were measured. The theory which was developed describes the combined effects of: 1) **depolymerization and hydrogen consumption;** 2) **crosslinking;** and 3) **external transport.** Recently, an expression to describe 4) **internal transport** has been added to the model. These processes, which are described below, are incorporated into a computer code which employs a Monte Carlo method for performing the statistical analysis.

1. **Depolymerization and Hydrogen Consumption** - A distributed kinetic rate about an average rate k_B described the random breaking of labile bridges. For the polymers, this kinetic rate (46) employs an activation energy which is in agreement with resonance stabilization calculations (71,72) and an overall rate which agrees with previous measurements on model compounds (73). The rate k_B determined for the breaking of ethylene bridges between naphthalene rings is in good agreement with the rate k_{tar} for tar formation from coal (6,13).

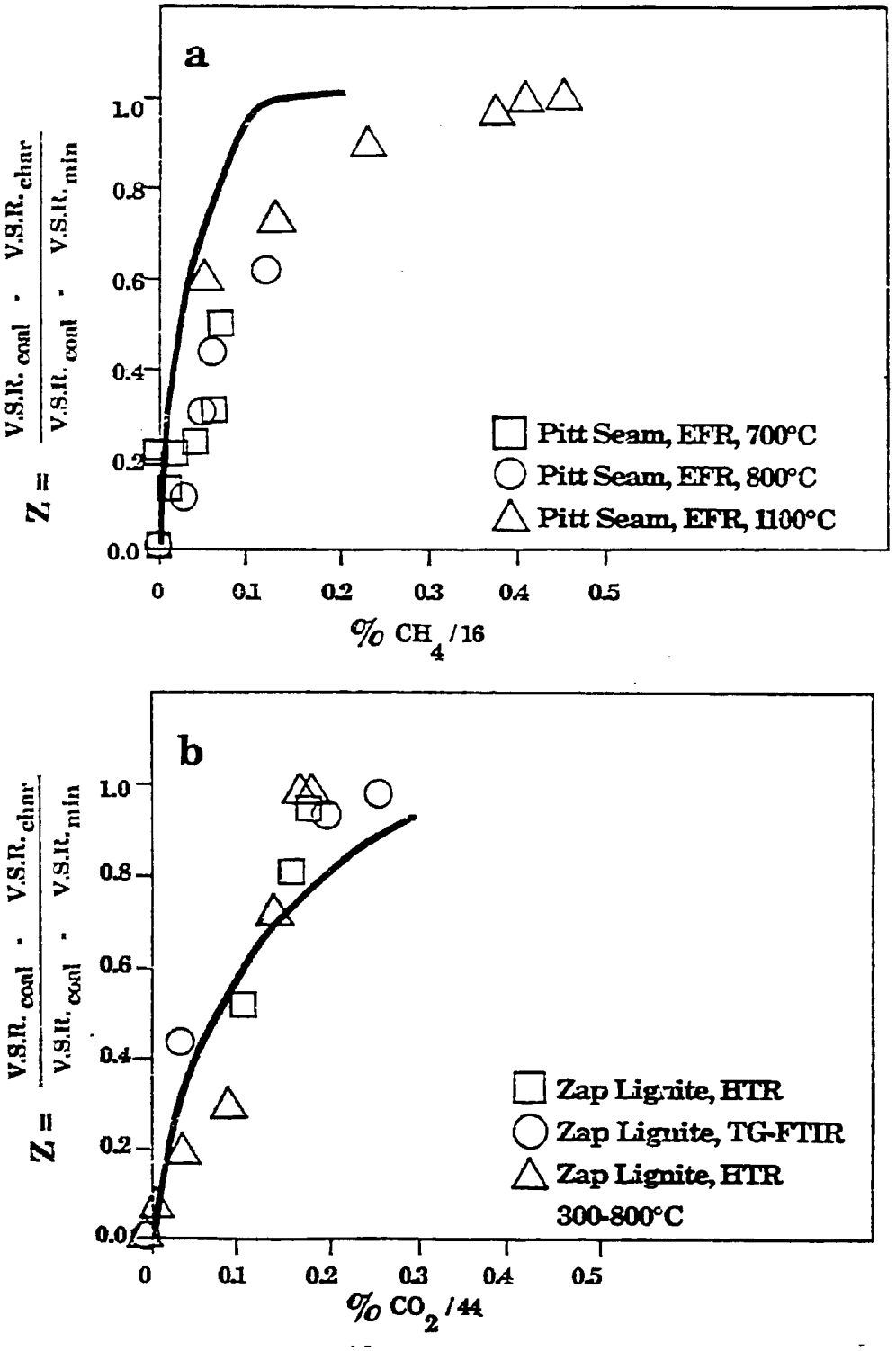

Figure 2. Measured and Calculated Normalized Volumetric Swelling Ratio (VSR), for Coal and Chars. a) Pittsburgh Seam Bituminous Coal Plotted Against the Methane Yield and b) Zap North Dakota Lignite Plotted Against CO_2 Yield. $V.S.R._{min}$ is the Value Achieved when Crosslinking is Complete. The Chars were Prepared in an Entrained Flow Reactor (EFR), a Heated Tube Reactor (HTR), and a Thermogravimetric Analyzer with Evolved Product Analysis by FT-IR (TG-FTIR). Described in Ref. 59. Reprinted from Ref. 63 with permission.

While crosslinking reactions were originally included in the DVC model using adjustable parameters for the rate and amount (30,31,46), work has recently been performed to define the reactions which cause crosslinking (33,63,74). Under the assumption that the crosslinking reactions may also release gas species, the molecular weight between crosslinks or crosslink density was correlated with the observed evolution of certain gas species during pyrolysis. Likely candidates were CO_2 formation from carboxyl groups or methane formation from methyl groups. Suuberg at al. (57) also noted that crosslinking in low rank coals is correlated with CO_2 evolution. Both reactions may leave behind free radicals which can be stabilized by crosslinking. Condensation of hydroxyl groups to form water and an ether link is also a possible reaction.

For a series of chars, the loss of volumetric swelling ratio in pyridine was compared with CO_2 evolution for a North Dakota (Beulah) lignite and CH_4 evolution for a Pittsburgh Seam bituminous coal (63). The results are presented in Fig. 2 (from Ref. 63). The abscissa (parameter Z), which is the change in volumetric swelling ratio (VSR) between coal and char divided by the maximum change is given by:

$$Z = (VSR_{coal} - VSR_{char})/(VSR_{coal} - VSR_{min})$$

Z is 0 for coal and 1 for fully crosslinked char. Since the lignite reaches maximum crosslinking before the start of methane evolution and the Pittsburgh Seam bituminous coal evolves little CO_2, correlations can be made separately between crosslinking and CO_2 evolution in the lignite and crosslinking and CH_4 evolution in the Pittsburgh seam bituminous coal. On a molar basis, the evolution of CO_2 from the lignite and CH_4 from the bituminous coal appear to have similar effects on the volumetric swelling ratio. The results suggest that one crosslink is formed for

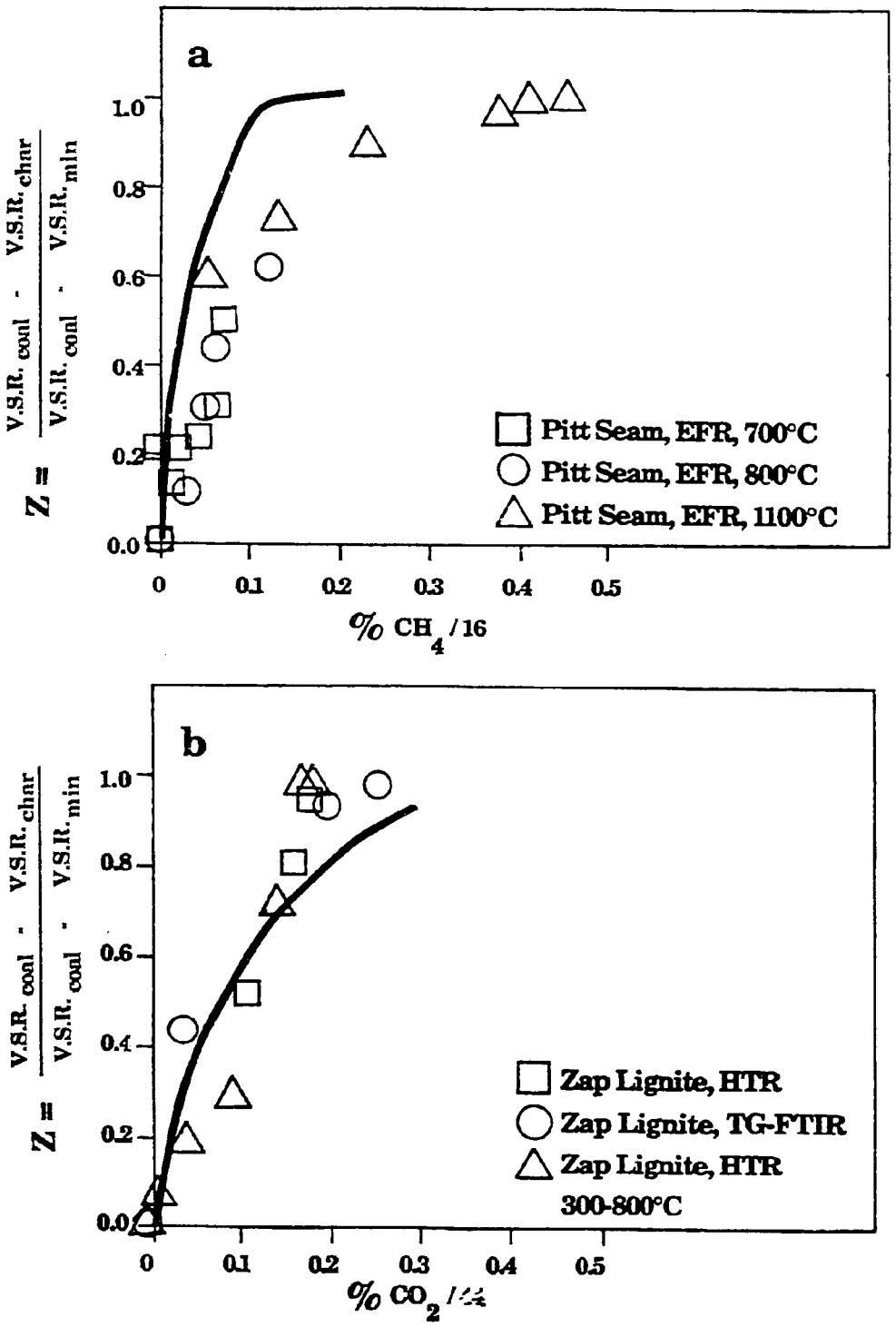

Figure 2. Measured and Calculated Normalized Volumetric Swelling Ratio (VSR), for Coal and Chars. a) Pittsburgh Seam Bituminous Coal Plotted Against the Methane Yield and b) Zap North Dakota Lignite Plotted Against CO_2 Yield. $V.S.R._{min}$ is the Value Achieved when Crosslinking is Complete. The Chars were Prepared in an Entrained Flow Reactor (EFR), a Heated Tube Reactor (HTR), and a Thermogravimetric Analyzer with Evolved Product Analysis by FT-IR (TG-FTIR). Described in Ref. 59. Reprinted from Ref. 63 with permission.

each CO_2 or CH_4 molecule evolved. No correlation was observed between the volumetric swelling ratio and tar yield for either coal. A correlation with water yield appears valid for the North Dakota (Beulah) lignite, but not for the Pittsburgh Seam bituminous coal.

It therefore appears that a correlation exists between gas evolution and crosslinking, which permits the rates for crosslinking and the number of crosslink sites to be related to rates and yields for gas evolution. The model assumes the following expression for the rate of increase of the number of crosslinks, m per gram

$$dm/dt = N_o\left[\frac{dW_{CO2}(gas)/dt}{44} + \frac{dW_{CH4}(gas)/dt}{16}\right] \qquad (2)$$

where the rates dW_i/dt per gram of coal of evolution of CO_2 and CH_4 are calculated in the FG subroutine. N_o is Avogadro's number.

3. **External Transport** - External transport from the particle surface to the bulk gas is by vaporization and diffusion through a gas boundary layer. The model of Unger and Suuberg (23) was originally employed. The modified expression for the vaporization law of Suuberg et al. (32) is now used to replace that in the original model. The rate of evolution per gram of coal $(dn_j/dt)_{ET}$ of oligomers of molecular weight M_j is given by

$$(dn_j/dt)_{ET} = (3/r_o^3\rho)rD_j X_j (P_j^s/RT) \qquad (3)$$

where r is the particle radius and r_o is the initial partial radius, ρ is the particle density, X_j is the mole fraction of species of molecular weight M_j in the metaplast, P_j^s is the vapor pressure for oligomers of molecular weight M_j, D_j is the

diffusivity of species of molecular weight M_j, R is the gas constant and T is the particle temperature.

4. Internal Transport - When comparing the predictions of the model to available data it was found that tar yields were overpredicted when devolatilization occurred at low temperatures. This was observed for either low heating rate experiments (6) or experiments with rapid heating to relatively low temperatures (16). As discussed in the Results Section, it appears that the lower yields were the result of the additional transport limitations within the particle. For softening coals, the transport mechanisms include: i) the transit of bubbles containing tar from the interior of the particle to the surface; ii) the transport of tars within the liquid to the bubble; iii) the stirring action of the bubble. For non-softening coals transport occurs by convection and diffusion within the pores. In the absence of sufficient information to accurately model these processes, the assumption was made that tars are carried out of the particle in the light devolatilization products (33) which exit the coal via bubbles or pores. The upper limit for this process is achieved if the heavier tars are at their equilibrium vapor pressure in the light gases. Then the rate of transport is proportional to the volume of light gases evolved which in turn is inversely proportional to the pressure within the particle $P_o + \Delta P$ where P_o is the ambient pressure and ΔP is the average pressure difference in the particle. Then,

$$(dn_j/dt)_{IT} = P_j^s X_j \sum_{\text{light products}} (dn_i/dt)_{chem} \left[\frac{1}{P_o + \Delta P} \right] \qquad (4)$$

where $(dn_j/dt)_{IT}$ is the internal transport rate per gram of coal for tar component j. $\sum_{\text{light products}} dn_i/dt)_{chem}$ is the rate of production per gram of coal of component i summed over all gas and tar species with molecular weight less than 300 amu. P_j^s

is the equilibrium vapor pressure for component j (given by Suuberg et al. (32)) and X_j is the mole fraction of component j in the metaplast. For the highly fluid Pittsburgh Seam bituminous coal, we have considered the upper limit to this rate where $P_o >> \Delta P$. Then all the terms in Eq. 4 can be determined by the combined FG-DVC model. ΔP is proportional to the coal's viscosity and so, will become important for less fluid coals. It is also important when P_o is small.

The effective rate for tar transport $(dn_j/dt)_{EFF}$ is calculated by assuming that the resistances to internal and external transport occur in series,

$$1/(dn_j/dt)_{EFF} = 1/(dn_i/dt)_{IT} + 1/(dn_i/dt)_{ET}$$

Schematic Representation of DVC Model - In the current DVC model, the parent coal is represented as a two-dimensional network of monomers linked by strong and weak bridges as shown in Fig. 3a. Condensed ring clusters are represented as monomers linked to form an oligomer of length "ℓ" by breakable and non-breakable bridges. The clusters are represented by circles with molecular weights shown in each circle. The molecular weight distribution of the monomers is assumed to be Gaussian and is described by two parameters M_{avg} (mean) and σ (standard deviation). The breakable bridges (assumed to be ethylene) are represented by single lines, the unbreakable bridges by double lines. "m_o" crosslinks per gram are added so that the molecular weight between crosslinks, M_c corresponds to the value reported in the literature (75) for coals of similar rank. Unconnected "guest" molecules (the extract yield) are obtained by choosing the value of ℓ. The ratio of ethylene bridges (two donatable hydrogens per bridge) to non-breakable bridges (no donatable hydrogens) is chosen to obtain the appropriate value for total donatable hydrogen.

The parameters M_c, ℓ, M_{avg} and σ determine the molecular weight distribution

of oligomers in the starting coal molecule. A histogram showing the distribution created by randomly picking monomers to form oligomers of length, ℓ and randomly crosslinking than to achieve an average molecular weight M_c between crosslinks is presented at the right of Fig. 3a. The distribution is divided into a pyridine insoluble portion below 3000 AMU (light shading) and a pyridine insoluble portion above 3000 AMU (dark shading). The parameters employed for a Pittsburgh Seam coal and North Dakota lignite are presented in Table I.

Figure 3b shows the molecule during pyrolysis. Some bonds have broken, other bonds have been converted to unbreakable bonds by the abstraction of hydrogen to stabilize the free radicals and new crosslinks have been formed. To determine the change of state of the computer molecules during a time step, the number of crosslinks formed is determined using the FG subroutine, and passed to the DVC subroutine. These crosslinks are distributed randomly throughout the char, assuming that the crosslinking probability is proportional to the molecular weight of the monomer. Then the DVC subroutine breaks the appropriate number of bridging bonds and calculates the quantity of tar evolved for this time step using the internal and external transport equations. The result is the coal molecule representation and the molecular weight distributions shown in Fig. 3b. The lighter "tar molecules", which leave the particle according to the transport equations, are shown as cross hatched. A fraction of the abstractable hydrogen is used to stabilize the free radicals formed by bridge breaking, creating two new methyl groups per bridge and the same fraction of breakable bridges is converted into (unbreakable) double-bonds.

Figure 3c shows the final char which is highly crosslinked with unbreakable bonds and has no remaining donatable hydrogen. The histogram now shows only tar and pyridine insoluble fractions. The extractables have been eliminated by tar

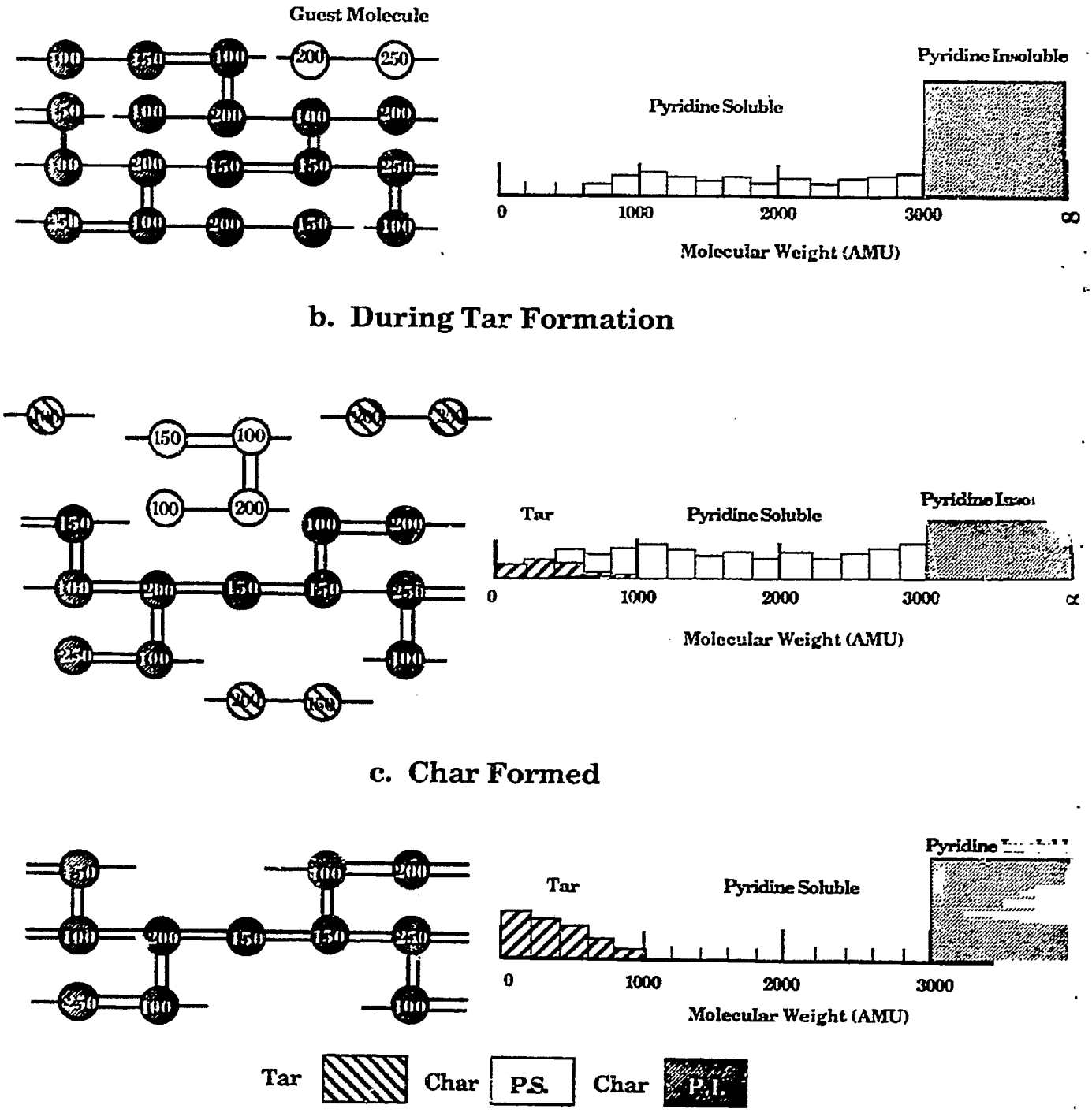

Figure 3. Representation of Coal Molecule in the DVC Simulation and Corresponding Molecular Weight Distribution. In the Molecule, the Circles Represent Monomers (ring clusters and peripheral groups). The Molecular Weight Shown by the Numbers is the Molecular Weight of the Monomer including the attached Bridges. The Single Line Bridges are Breakable and can Donate Hydrogen. The Double Line Bridges are Unbreakable and do not Donate Hydrogen. The Molecular Weight Distribution of the Coal, Tar, and Chars are shown as a Histogram at the Right. The Histogram is Divided into Tar and Char with Pyridine Soluble and Insoluble Fractions.

Table I

PARAMETERS FOR DVC MODEL

	Concentrations	Pittsburgh Seam	Zap Lignite
Labile Bridges	W_B	0.094	0.082
Nuclei (ring clusters) *	W_N From FG Model	0.562	0.440
Peripheral Groups (sources for gases)	W_P From FG Model	0.344	0.478
Donatable Hydrogens	(2/28) W_B	0.0067	0.0059
Oligomer Length	l #/oligomer	7	10
Molecular Weight between Crosslinks	M_c, gms/gmole	2900	1400

MOLECULAR WEIGHTS

Labile Bridges	Fixed at 28	28	28
Monomers	Gaussians Distribution-$M_{avg},(\sigma)$	256,(250)	256,(250)
Gas	From FG Model		
Tar	Predicted in Model from Vaporization Law		
Non-labile Bridges	Fixed at 26	26	26

* Carbon in aromatic rings plus non-liable bridges

formation and crosslinking.

The output of the DVC subroutine is the molecular weight distribution in the coal, its time dependent transformation during devolatilization and the separation of tar determined by the transport of the lighter components.

Functional Group (FG) Model Formulation

The Functional Group (FG) model has been described in a number of publications (5,6,11-13). It permits the detailed prediction of volatile species concentrations (gas yield, tar yield and tar functional group and elemental composition) and the chemical and functional group composition of the char. It employs coal independent rates for the decomposition of individual assumed functional groups in the coal and char to produce gas species. The ultimate yield of each gas species is related to the coal's functional group composition. Tar evolution is a parallel process which competes for all the functional groups in the coal. In the original FG model, the ultimate tar yield is an input parameter which is adjusted for each type of experiment. The DVC subroutine provides this parameter.

Schematic Representation of FG Model - The mathematical description of the functional group pyrolysis model has been presented previously (5,6,11-13). The evolution of tar and light gas species provides two competing mechanisms for removal of a functional group from the coal: evolution as a part of a tar molecule and evolution as a distinct gas species. This process is shown schematically in Fig. 4. To model these two paths, with one path yielding a product which is similar in composition to the parent coal, the coal is represented as a rectangular area with X and Y dimensions. As shown in Fig. 4a, the Y dimension is divided into fractions according to the chemical composition of the coal. Y_i^0 represents the

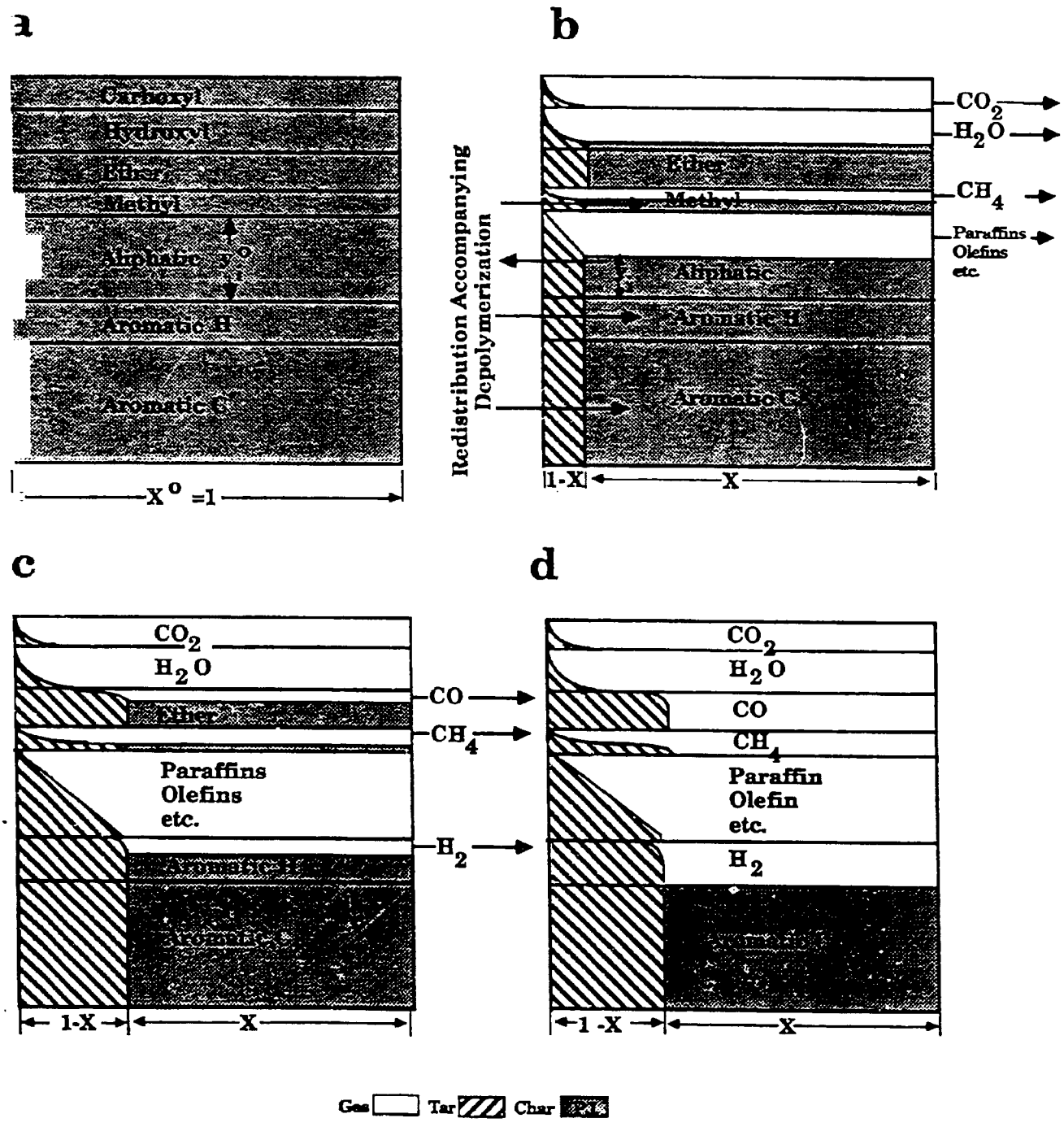

Figure 4. Schematic Representation of Functional Group (FG) Model. a) Initial Coal Composition, b) During Tar Formation, c) Completion of Tar Formation, and d) Completion of Devolatiiization.

initial fraction of a particular component (carboxyl, aromatic hydrogen, etc.) and the sum of the Y_i^o's equal one. The evolution of each component into the gas (carboxyl into CO_2, aromatic hydrogen into H_2, etc.) is represented by the first-order diminishing of the Y_i dimension, $dY_i/dt = -k_i Y_i$.

The X dimension is divided into char X and tar (1-X); initially X = 1. The evolution of the tar is represented by the decreasing of the X dimension, dX/dt, computed in the DVC subroutine as

$$\frac{dX}{dt} = -\sum_j (dn_j/dt)_{EFF} M_j$$

The fractional amount of a particular functional group component in the char is

$$W_i(char) = X \cdot Y_i$$

and the amounts in the gas and tar may be obtained by integration with respect to time starting from t = 0:

Secondary reactions such as further decomposition of aliphatic species to form olefins, acetylene, and soot modify the basic equations. Some of these have been described elsewhere (6).

Figure 4a shows the initial state of the coal. Values for Y_i^o are obtained from elemental analysis, FT-IR analysis of the raw coal and from analysis of the products of one or two pyrolysis experiments. Figure 4b shows the initial stage of devolatilization, during which the most volatile components, H_2O, CO-loose, and CO_2 evolve from the hydroxyl, ether-loose, and carboxyl groups, respectively, along with aliphatics and tar. At a later stage (Fig. 4c) CO-tight, HCN and H_2 are evolved from the ether-tight, ring nitrogen, and aromatic hydrogen. Figure 4d shows the final state of the char, tar and gas.

The evolution of gas and the composition of the char and tar are then

described mathematically as follows:

5. Gas Formation - The evolution of each gas species is assumed to be a first order reaction,

$$dW_i(gas)/dt = k_i W_i(char) = k_i X Y_i \qquad (5)$$

where, $dW_i(gas)/dt$ is the rate of evolution of species i into the gas phase, k_i is a distributed rate for species i and $W_i(char)$ is the functional group source remaining in the char. The concept of the distributed rate was introduced by Pitt (76) and subsequently employed by Rennhack (77) and Anthony et al. (22) to describe weight loss. Hanbaba et al. (78), Juntgen and van Heek (79), and Weimer and Ngan (9) employed distributed rates for individual species. In the FG subroutine, k_i is given by an Arrhenius expression $k_i = k_i^o \exp(-(E_i \pm \sigma_i)/RT)$ where $\pm \sigma_i$ indicates that a Gaussian distribution is employed to describe the product sources $W_i(E_i)$ as a function of the activation energies E_i (5,9,12,22). $W_i(E_i) = (W_I^o/\sqrt{\sigma_i}\sqrt{2\pi})\exp(-(E_i-E_I^o)^2/2\sigma_i^2)$. E_I^o is the average activation energy and σ_i is the width of the Gaussian distribution. Note that $W_i(char)$ also is decreased by evolution of the source with the tar.

6. Tar Composition - The tar composition is tracked by summing the functional group contributions evolved with the tar. The rate of evolution of each contribution is:

$$dW_i(tar)/dt = -(dX/dt)Y_i \qquad (6)$$

where $dW_i(tar)/dt$ is the rate of evolution of each functional group component with the tar.

Table II. Kinetic Rate Coefficients and Species Composition Percents for Pittsburgh Seam Coal.[a]

composition parameters	gas	primary functional group source	rate equation	Pittsburgh No. 8 bituminous coal	North Dakota Zap Lignite
C		———	———	0.821	0.665
H		———	———	0.056	0.048
N		———	———	0.017	0.011
S(organic)		———	———	0.024	0.011
O		———	———	0.082	0.265
total		———	———	1.000	1.000
Y^o_1	CO_2 extra loose	carboxyl	$k_1 = 0.56E+18 \exp(-(29000\pm2000)/T)$	0.000	0.065
Y^o_2	CO_2 loose	carboxyl	$k_2 = 0.65E+17 \exp(-(33850\pm1500)/T)$	0.007	0.030
Y^o_3	CO_2 tight	———	$k_3 = 0.11E+16 \exp(-(38315\pm2000)/T)$	0.005	0.005
Y^o_4	H_2O loose	hydroxyl	$k_4 = 0.22E+19 \exp(-(30000\pm1500)/T)$	0.012	0.062
Y^o_5	H_2O tight	hydroxyl	$k_5 = 0.17E+14 \exp(-(32700\pm1500)/T)$	0.012	0.033
Y^o_6	CO ether loose	———	$k_6 = 0.14E+19 \exp(-(40000\pm6000)/T)$	0.050	0.060
Y^o_7	CO ether tight	ether O	$k_7 = 0.15E+16 \exp(-(40500\pm1500)/T)$	0.021	0.038
Y^o_8	HCN loose	———	$k_8 = 0.17E+14 \exp(-(30000\pm1500)/T)$	0.009	0.007
Y^o_9	HCN tight	———	$k_9 = 0.69E+13 \exp(-(42500\pm4750)/T)$	0.023	0.013
Y^o_{10}	NH_3	———	$k_{10} = 0.12E+13 \exp(-(27300\pm3000)/T)$	0.000	0.001
Y^o_{11}	CH_x aliphatic	H(al)	$k_{11} = 0.84E+15 \exp(-(30000\pm1500)/T)$	0.207	0.102
Y^o_{12}	methane extra loose	methoxy	$k_{12} = 0.84E+15 \exp(-(30000\pm1500)/T)$	0.020	0.000
Y^o_{13}	methane loose	methyl	$k_{13} = 0.75E+14 \exp(-(30000\pm2000)/T)$	0.015	0.017
Y^o_{14}	methane tight	methyl	$k_{14} = 0.34E+12 \exp(-(30000\pm2000)/T)$	0.015	0.009
Y^o_{15}	H aromatic	H(ar)	$k_{15} = 0.10E+15 \exp(-(40500\pm6000)/T)$	0.013	0.017
Y^o_{16}	methanol	———	$k_{16} = 0.00E+00 \exp(-(30000\pm0)/T)$	0.000	0.000
Y^o_{17}	CO extra tight	ether O	$k_{17} = 0.20E+14 \exp(-(45500\pm1500)/T)$	0.020	0.090
Y^o_{18}	C nonvolatile	C(ar)	$k_{18} = 0$	0.562	0.440
Y^o_{19}	S organic	———	———	0.024	0.011
					1.000
Y^o	tar	———	$k_T = 0.86E+15 \exp(-(27700\pm1500)/T)$	1.000	

a. The Rate Equation is of the form $k_n = k_0 \exp(-(E/R)\pm(\sigma R))/T$, with k_0 in s^{-1}, E/R in K, and σ/R in K.

7. Char Composition - The change in the ith char pool, $W_i(char)$ is computed by summing the losses to the gas and tar and the redistributions determined in the DVC subroutine,

$$dW_i(char)/dt = -dW_i(gas)/dt - dW_i(tar)/dt + dW_i(DVC)/dt \qquad (7)$$

where $dW_i(DVC)/dt$ are the source and loss terms from the DVC model, given by $(30/28)k_B W_B$, $(2/28)k_B W_B$, $(24/28)k_B W_B$ and $-2k_B W_B$ for methyl, aromatic H, aromatic C, and labile bridge functional groups, respectively.

The general rates and specific composition parameters for Pittsburgh Seam coal and North Dakota lignite are presented in Table II.

SUMMARY OF THE FG-DVC MODEL

The various processes described by the general model are summarized in Tables III and IV. The four processes, 1) **depolymerization and hydrogen consumption**, 2) **crosslinking**, 3) **external transport**, and 4) **internal transport**, are described by the DVC subroutine and the three processes, 5) **gas formation**, 6) **tar composition**, and 7) **char composition** are described by the FG subroutine. The coupling of the two portions of the model occurs in five places: a) the rate of mass loss to the tar is determined in the DVC subroutine and passed to the FG subroutine as an effective rate k^*_{tar}; b) the depolymerization reaction is accompanied by a redistribution of the functional group compositions. The DVC subroutine provides loss terms for the labile bridge component and source terms for the methyl, aromatic hydrogen, and aromatic carbon components; c) the crosslinking in the DVC subroutine is determined by the rate of CO_2 and CH_4 evolution computed by the FG subroutine, one crosslink formed for each molecule evolved; d) the evolution of light gas species from the FG subroutine determines the internal transport of tar

TABLE III

SUMMARY OF PROCESSES CONSIDERED IN THE DAC PORTION OF THE GENERAL DEVOLATILIZATION MODEL

PROCESS	REACTION	PARAMETERS	OBSERVABLES
1. **Depolymerization and Hydrogen Consumption** - breaking of weak bonds in the coal macro-molecule to form smaller molecular fragments and stabilization of the fragments by hydrogen donation.	First order breaking of labile bridges W_β ($\phi CH_2-CH_2-\phi$) in the coal or char (see Eq. 1). Each broken bridge is accompanied by the utilization of four donatable hydrogens (aliphatic or hydroaromatic) for the conversion of two methylene groups into methyl groups and two aliphatic CH_2 groups to aromatic CH groups.	**Coal Dependent** - Weight percentage of labile bridges in coal W_β. **Coal Independent** - Kinetic rate for bond breaking $k_\beta = k_\beta^0 \exp((E_\beta \pm \sigma_\beta)/RT)$.	Changing extract yield in coal and char. Evolution of tar. Changing aliphatic, aromatic and methyl hydrogen concentration of the coal and char.
2. **Crosslinking Repolymerization** - of the coal macromolecule and molecular fragments.	Formation of crosslinks equated with the evolution of CO_2 and CH_4 (one crosslink is formed for each gas molecule involved) (see Eq. 2).	**Coal Dependent** - Number of potential crosslink sites W_{CO2}^0 and W_{CH4}^0 from gas formation parameters. **Coal Independent** - Rates k_{CO2} and k_{CH4} from gas formation parameters.	Changing volumetric swelling ratio of the coal and char. Changing extract yield in char.
3. **External Transport** - from particles surface to bulk gas of molecular fragments and guest molecules.	Vaporization and diffusion through the gas boundary layer employing the model of Unger and Suuberg (2) and the vaporization law of Suuberg et al. (30) (see Eq. 3).	**Coal Independent** - Molecular weight dependent vapor pressure and diffusion law.	Tar molecular weight distribution. Variation of tar yield and molecular weight distribution with heating rate, final temperature, and pressure.
4. **Intraparticle Transport** - of molecular fragments and guest molecules.	Tar is transported in light gas species at the equilibrium vapor pressure of the tar molecule (see Eq. 4).	**Coal Dependent** - Pressure gradient ΔP i.. the particle. **Coal Independent** - Molecular weight dependent vapor pressure law (30).	Tar molecular weight distribution. Variation of tar yield and molecular weight distribution with heating rate, final temperature, and pressure.

TABLE IV

SUMMARY OF PROCESSES CONSIDERED IN THE FG PORTION OF THE GENERAL DEVOLATILIZATION MODEL

5. **Gas Formation** - formation of gas species "i" Major Species CO_2 (3 reactions) CO (3 reactions) H_2O (2 reactions) CH_4 (2 reactions) H_2 (1 reaction) Paraffins (1 reaction) Olefins (1 reaction)	First order evolution from source W_I in the coal and char (see Eq. 5). Source Carboxyl Ether Hydroxyl Methyl Aromatic hydrogen Aliphatic CH Aliphatic CH	**Coal Dependent** - Weight Percent of source in coal $W_I^0 = Y_I^0$. **Coal Independent** - Kinetic rates $k_I = k_I^0 \exp((E_I \pm \sigma_I)/RT)$	Evolution of gases CO_2, CO, H_2O, CH_4, H_2, paraffins, olefins
6. **Tar Composition** - determined by the sum of i functional groups.	Each tar functional group component evolves at a rate equal to the instantaneous functional group composition in the char times the overall rate of tar evolution from the DVC model (see Eq. 6)	**Coal Dependent** - Weight percent of source in coal $W_I^0 = Y_I^0$. **Coal Independent** - Kinetic rate for bond breaking k_{II}.	Tar elemental and functional group composition.
7. **Char Composition** - determined by the sum of i functional groups.	The rate of change in each functional group is equal to the loss of tar and gas plus the redistribution from the DVC model (see Eq. 7).	**Coal Dependent** - Weight percent of source in coal $W_I^0 = Y_I^0$. **Coal Independent** - k_I's and k_B.	Char elemental and functional group composition.

by Eq. 4; e) the evolution of the peripheral groups reduces the molecular weight of the oligomers. Presented below (Fig. 5) is a schematic of the linked model for a simple case of only one gas species. Also presented is a summary of the FG-DVC model assumptions.

Schematic of FG-DVC Model

The combined model connects the upper (DVC portion) and lower (FG portion) parts of Figs. 5a-5d. The model is initiated by specifying the Functional Group composition parameters (W_B, W_N and in this case only one gas species parameter, W_g) and the coal structure parameters (number of breakable bridges, starting oligomer length ℓ, number of added crosslinks, m_o, and the monomer molecular weight distribution parameters M_{avg} and σ). The starting molecular weight distribution of oligomers is presented at the top of Fig. 5a. The monomers are assumed to have the average elemental and functional group composition given by the FG parameters. The functional groups are divided into pyridine soluble and pyridine insoluble parts. Each computer simulation considers coal to consist of 50-100 molecules made from 2100-2400 monomers. The model has been programmed in Fortran 77 and runs on Apollo DN580 and Sun Microsystems 3/260 and 3/50 computers.

Once the starting distriubtion of oligomers in the coal is established, it is then subjected to a time-temperature history made up of a series of isothermal time steps. During each step, the gas yields, elemental composition and functional group compositions are computed using the FG subroutine. The molecular weight distribution, the escape of tar molecules and the re-distribution of hydrogens and carbons from the labile groups is computed with the DVC subroutine. Figure 5b illustrates tar formation simultaneous with gas formation. The labile bridges are either evolved with the tar, converted to methyl groups (and thus added to the peripheral groups) or converted to unbreakable bridges (and thus added to aromatic

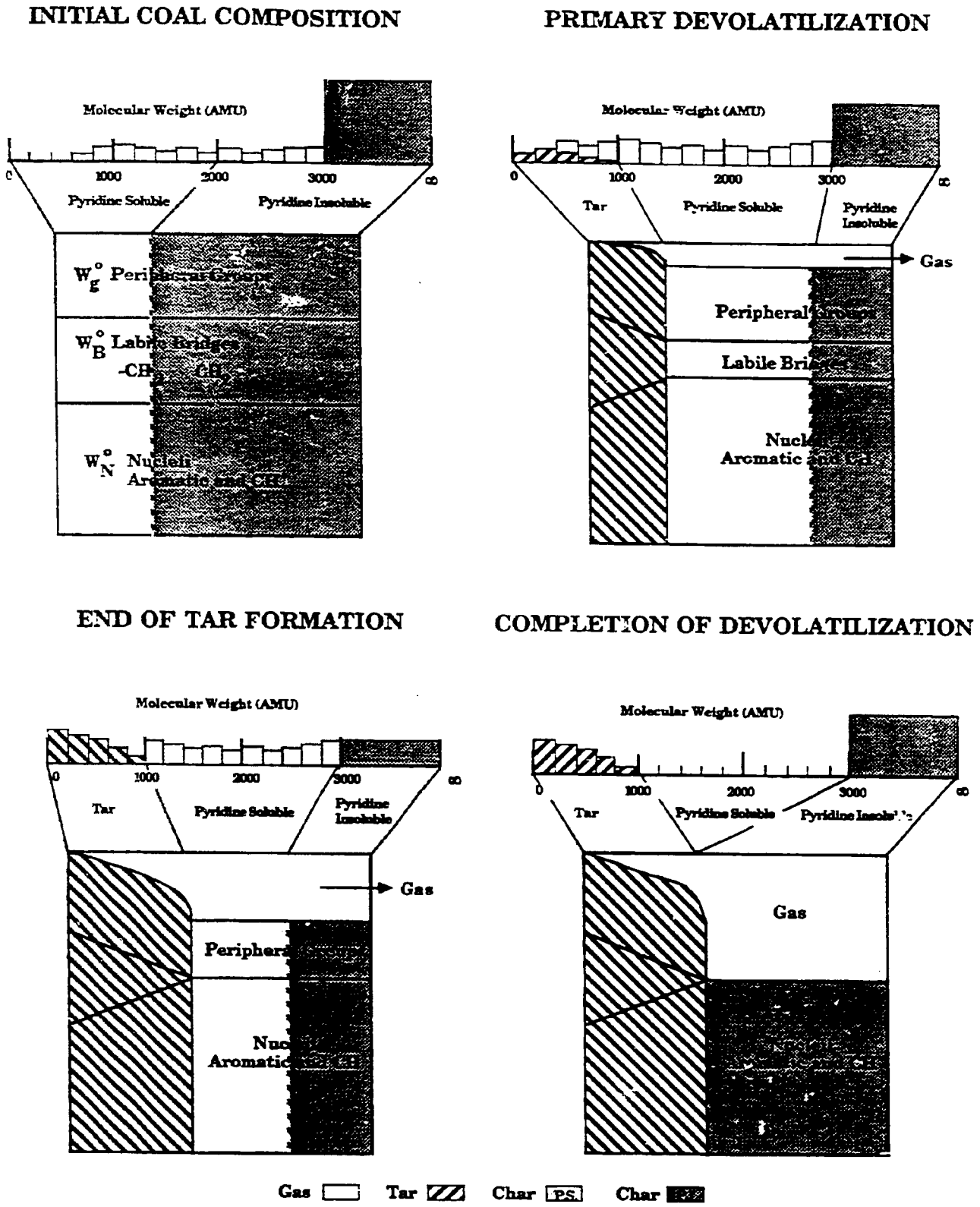

Figure 5. Schematic Representation of the FG-DVC Model Combining the DVC and FG Subroutines. The FG Subroutine is Illustrated for a Single Gas Species Only.

and CH groups). Tar formation is complete (Fig. 5c) when all the labile bridges are consumed. Devolatilization is completed (Fig. 5d) when all volatile functional groups (in this case the peripheral groups) are removed from the char.

A typical simulation for a complete time temperature history takes about 2 minutes on the Sun 3/260 computer.

Summary of FG-DVC Model Assumption

FG Subroutine Assumptions:

(a) Light gas species are formed from the decomposition of specific functional groups with rate coefficients which depend on the functional group but are insensitive to coal rank. The evolution rate is first order in the remaining functional group concentration in the char. The rates follow an Arrhenius expression with a Gaussian distribution of activation energies (5,12,22).

(b) Simultaneous with the production of light gas species, is the thermal cleavage of bridge structures in the coal to release molecular fragments of the coal (tar) which consist of a representative sampling of the functional group ensemble. The instantaneous tar yield is given by the DVC subroutine.

(c) Under conditions where pyrolysis products remain hot (such as an entrained flow reactor), pyrolysis of the functional groups in the tar continues at the same rates used for functional groups in the char, (e.g., the rate for methane formation from methyl groups in tar is the same as from methyl groups in the char).

DVC Subroutine Assumptions:

(d) The oligomer length, ℓ, the number of crosslinks, m_o, and the number of unbreakable bonds are parameters of the model, chosen to be consistent with the coal's measured extract yield, crosslink density and donatable hydrogen concentration.

(e) The molecular weight distribution is adjusted so that the model predictions fit the observed molecular weight distribution for that coal, measured by pyrolysis of the coal (in vacuum at 3°C/min to 450°C) in a FIMS apparatus (58). Molecular weights 106, 156, 206, 256, 306, 356 and 406 (which are 1,2,3,4,5,6 and 7 aromatic ring compounds with two methyl substituents) are considered as representative of typical monomer molecular weights.

(f) During pyrolysis, the breakable bonds are assumed to rupture randomly at a rate k_β, described by an Arrhenius expression with a Gaussian distribution of sources as a function of activation energies. Each rupture creates two free radicals which consume two donatable hydrogens to form two new methyl groups and convert two more donatable hydrogens to two aromatic CH groups. Oxymethylene bridges which may be important for low rank coals have not been modeled although a second class of labile bridges could easily be added.

(g) All the donatable hydrogens are assumed to be located in the labile bridges. Two donatable hydrogens are available at each bridge. The consumption of the donatable hydrogen converts the bridge into an unbreakable bridge by the formation of a double bond. The unbreakable bridges are included in the aromatic hydrogen and aromatic carbon functional groups.

(h) Tar formation continues until all the donatable hydrogens are consumed.

(i) During pyrolysis, additional unbreakable crosslinks are added at a rate determined by the evolution of CH_4 and CO_2. One crosslink is created for each evolved molecule. The rate of CH_4 and CO_2 evolution is given by the FG subroutine.

(j) The crosslinks are distributed randomly, with the probability of attachment on any one monomer being proportional to the molecular weight of the monomer.

(k) Tar molecules are assumed to be transported from the surface of the coal particle at a molecular weight dependent rate controlled by evaporation and gas phase diffusion away from the particle surface. The expressions derived by Unger and Suuberg (23) and using the revised vaporization law of Suuberg et al. (32) are employed.

(l) Internal transport resistance is assumed to add to the surface transport resistance. A simple empirical expression (Eq. 4) is used to describe bubble transport resistance in softening coals and convective transport through pores in non-softening coals.

(m) Extractable material (in boiling pyridine) in the char is assumed to consist of all molecules less than 3000 AMU. This can be adjusted depending on the solvent and extraction conditions.

(n) The molecular weight between crosslinks, M_c is computed to be the total molecular weight in the computer molecule divided by the total number of crosslinks. This assumption will underestimate M_c since broken bridges are not considered.

RESULTS

The model predictions have been compared to the results obtained from a number of experiments on the pyrolysis of a Pittsburgh Seam coal (6,7,16,22) and a North Dakota (Beulah) lignite (6,74). The coal composition parameters are presented in Tables I and II. It should be noted that different samples of Pittsburgh seam coal from different sources were employed. While the elemental compositions were similar, extract yields varied depending on the sample source. The oligomer length in Table I was chosen to fit an extract yield of 30%. Comparisons are considered for gas yields, tar yields, tar molecular weight distributions, extract yields and volumetric swelling ratio.

Volatile Yields

Extensive comparisons of the FG model with gas yields have been presented previously for high and low heating rate devolatilization experiment (5,6,11-13). The Functional Group parameters and the kinetic rates used for this work for the Pittsburgh Seam coal and North Dakota (Zap) lignite are principally those determined previously and published in Ref. 6. The methane parameters for the Pittsburgh Seam coal were, however, adjusted (methane X-L = 0.0, methane-L = 0.02, methane-T = 0.015, unchanged) to better match yield of Refs. 5,6 and 7 (see Fig. 20c in Ref. 6). Also note that the CH_x-aliphatic rate in Ref. 6 applies to the observed gas species (paraffins, olefins, C_2H_6, C_2H_4) only. The aliphatic material in the labile bridge part of the aliphatic group is assumed to be made up of bridges which volatilize only when attached to a tar molecule (i.e., $k_1 = 0$). Also the rate for CO_2-loose has been adjusted to improve the predictions of the change in tar molecular weight distributions with heating rate. The predictions of gas yield have not been changed noticeably.

As examples of the application of the FG model to predict volatile yields, Figs. 6 and 7 show a comparison of the model predictions with data taken at 0.5°C/sec for the lignite and bituminous coal. The slow heating rate experiment best illustrates the contribution from more than one reaction to several of the evolved species. These can be seen as more than one evolution peak per species. The peaks are labeled corresponding to the functional groups listed in Table II. The same kinetic parameters were employed to fit both samples; only the amounts of each functional group source differs. There is good agreement between the model prediction and the experimental results.

Extract Yields

Figure 8 compares the FG-DVC predictions to the data of Fong et al. (16) on total volatile yield and extract yield as a function of temperature in pyrolysis at 0.85 ATM. The experiments were performed in a heated grid apparatus at heating rates of approximately 500°C/sec, with variable holding times and rapid cool down. The predictions at the two higher temperatures (Figs. 8c and 8d) are in excellent agreement with the data. Having fixed all the rates and functional group compositions based on previous work, the only adjustable parameters were the number of labile bridges (which fixes the donatable hydrogen concentration) and the monomer distribution, assumed to be Gaussian.

Initially, the predictions for the two lower temperatures were not good when internal transport limitations were neglected. The dashed line in Fig. 8a shows the predicted yield in the absence of internal transport limitations (i.e., $(dn_j/dt)_{IT}$ (Eq. 4)$\gg$$(dn_j/dt)_{ET}$ (Eq. 3)). The predicted ultimate yield is clearly too high. The data suggest that the low yields are not a result of unbroken bonds (which would result from a lower bond breaking rate, k_B), since the extract yields

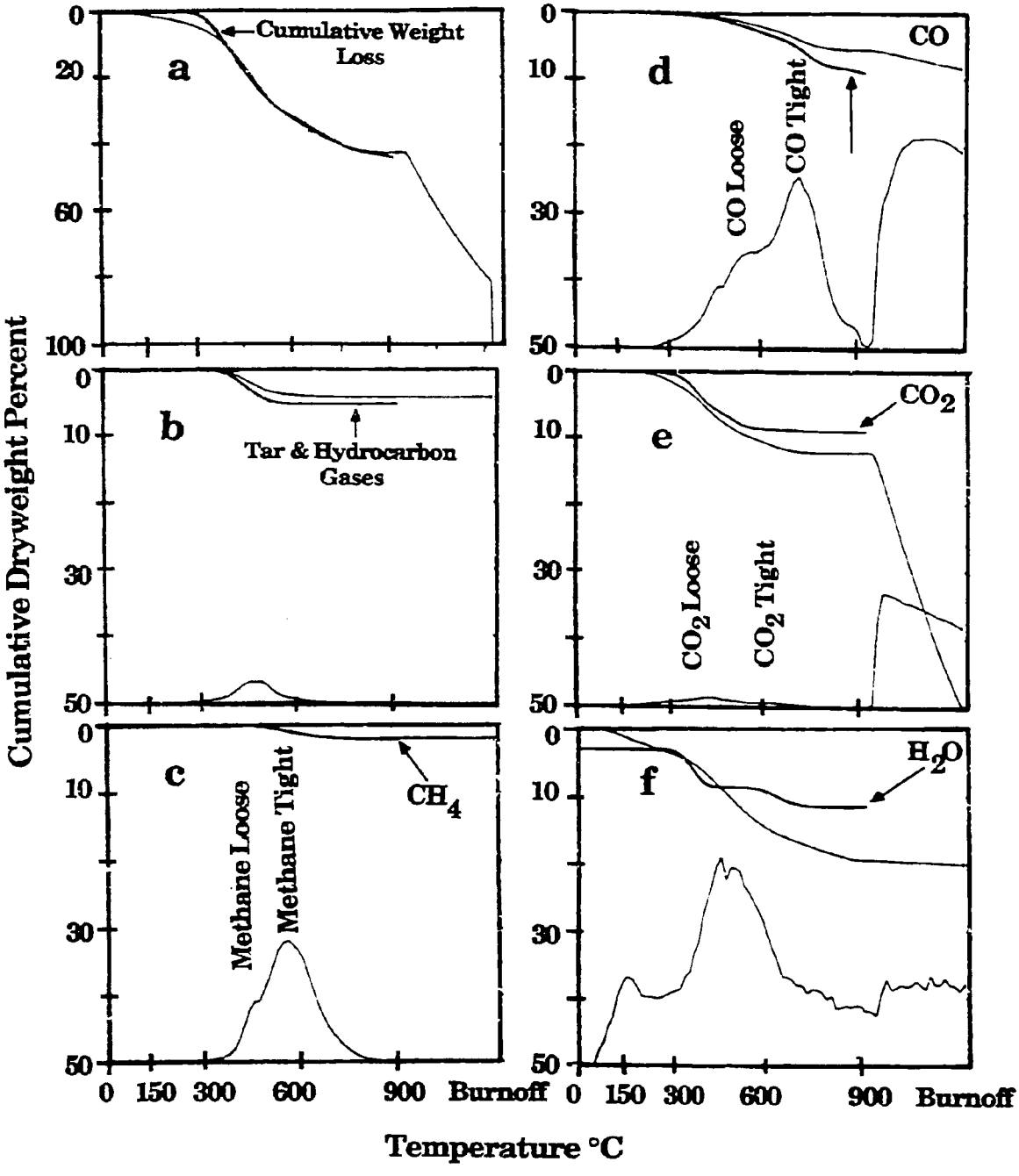

Figure 6. Pyrolysis Results for North Dakota Lignite, 200 x 325 mesh, Heated at 30 K/min (0.5 K/s) in the TGA/EGA. Upper Solid Lines are Cumulative Evolution Data and Predictions of the Functional Group Model for Cumulative Product Evolution. The Theory Lines are Indicated with Arrows. The Lower Solid Lines are Mass Evolution Rate Data (arbitrary scale). After the Coal Reaches 900°C, it is Quenched to 700°C and the Char is Oxidized for Elemental Analysis.

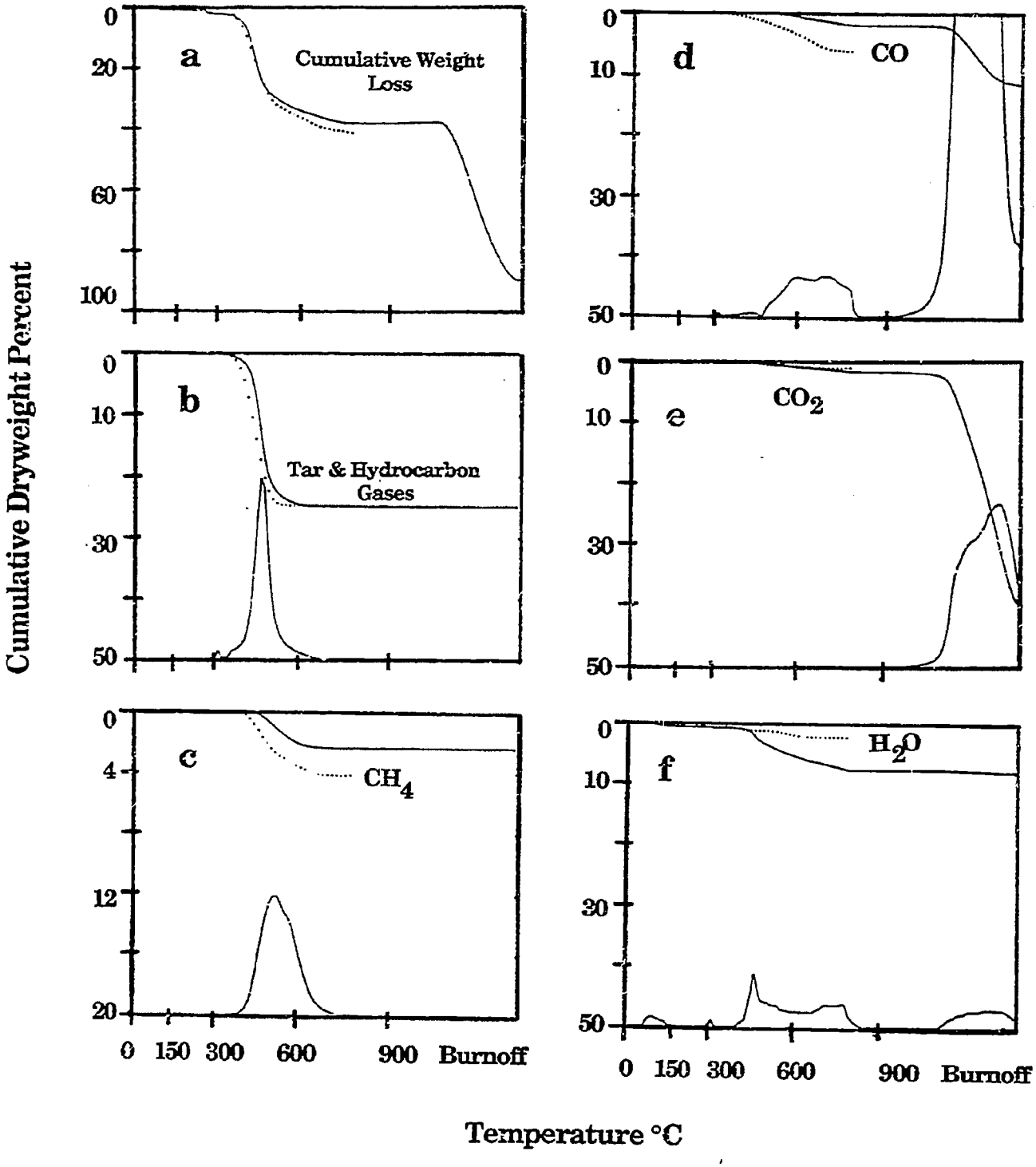

Figure 7. Pyrolysis Results for Pittsburgh Seam Bituminous Coal, 200 x325 mesh Heated at 30 K/min (0.5 K/s) in the TGA/EGA. Upper Solid Lines are Cumulative Evolution Data. Dotted Lines are Predictions of the Functional Group Model for Cumulative Product Evolution. The Theory Lines are Indicated with Arrows. The Lower Solid Lines are Mass Evolution Rate Data (arbitrary scale). After the Coal Reaches 900°C, it is Quenched to 700°C and the Char is Oxidized for Elemental Analysis.

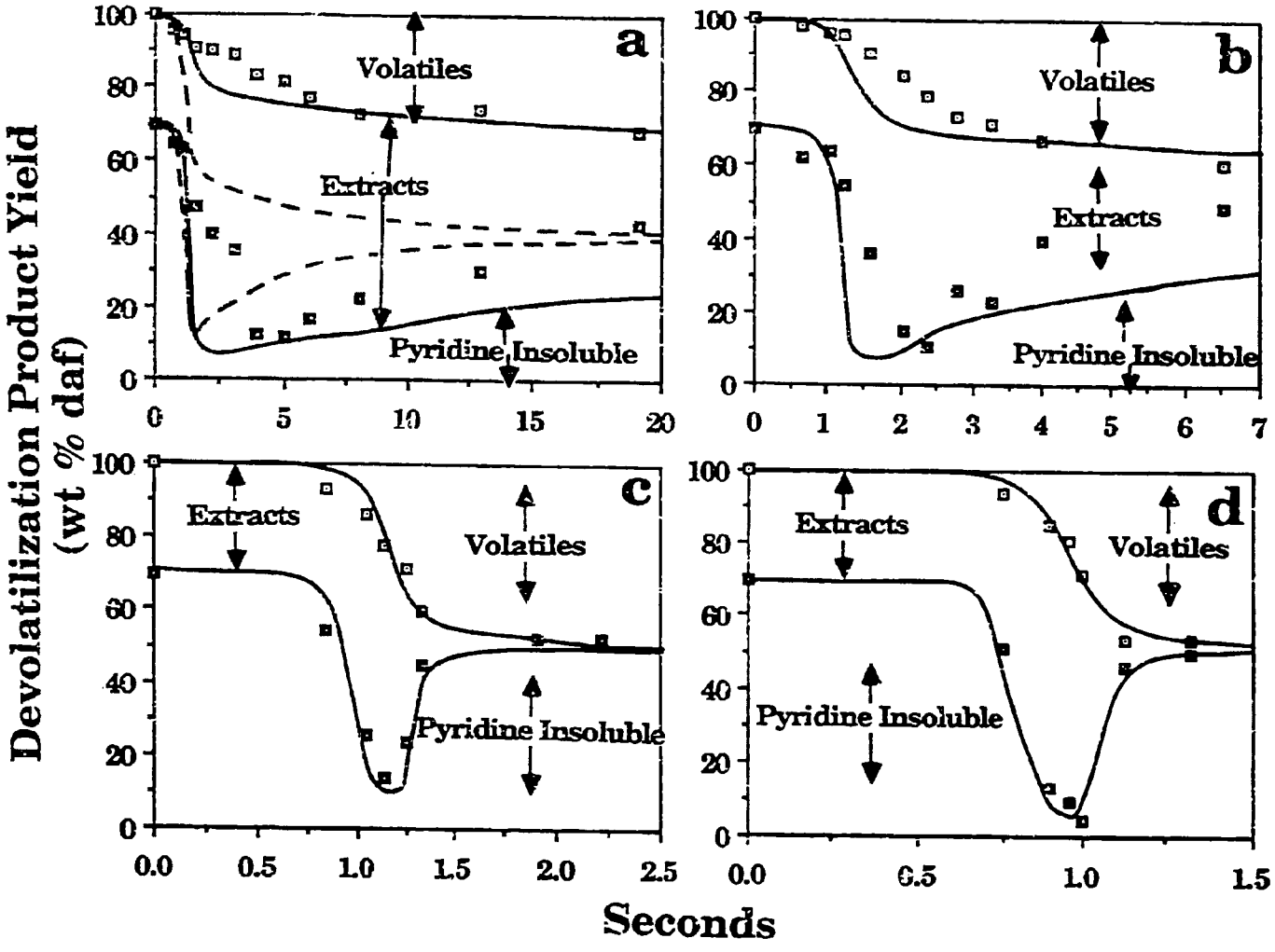

Figure 8. Comparison of FD-DVC Model Predictions (lines) with the data of Fong et al (16) (symbols) for Pittsburgh Seam Coal. a) 813K @ 470 k/s, b) 858K @ 446k/s, c) 992K @ 514k/s and d) 1018K @ 640k/s. P=0.85 atm. The Dashed Line in a Shows the Predicted Yield in the Absence of Internal Transport Limitations.

at low temperatures are equivalent to those at the higher temperatures. The low yields thus appear to be a result of an additional transport limitation.

Equation 4 was employed for the internal transport rate. The number of labile bridges then had to be slightly readjusted to match the 1018 K case. The predictions are the solid lines in Fig. 8. The internal transport limitation is important when pyrolysis occurs at low temperatures and $\sum_{light} dn_i/dt$ is small. It is much less important for the 1018 K and 992 K cases, making only a small difference in the predicted yields. Also, the use of Eq. 4 appears to predict the appropriate drop in tar yield at 0.5°C/sec (maximum value 17%) compared to 30% when devolatilization occurs at high temperature.

There still is a discrepancy between the prediction and the data at early times for the two lower temperatures (Figs. 8a and 8b). While it is possible that the rate k_B for bond breaking is too high, adjustment of this rate alone significantly lowers the extractable yield, since the lower depolymerization rate is closer to the methane crosslinking rate. In addition, both the methane and depolymerization rates appear to be in good agreement with the data at even lower temperatures, as shown in Figs. 6 and 7. Another possibility is that the coal particles heat more slowly than the nominal temperatures given by Fong et al. (16). Such an effect could be caused by having some clumps of particle which would heat more slowly than isolated particles, by reduction in the convective heat transfer due to the volatile evolution (blowing effect), or by endothermic tar forming reactions. A firm conclusion as to the source of this remaining discrepancy cannot be drawn without further investigation.

It is also seen in Figs. 8a and 8b that the crosslinking rate is higher than predicted. This can be due to other crosslinking events not considered. These

possibilities are currently under investigation.

Crosslink Density

To examine the effect of coal rank on crosslinking, the volumetric swelling ratios (VSR) for North Dakota (Beulah) lignite and Pittsburgh Seam bituminous coal were measured as a function of temperature for the same time-temperature history used in Figs. 6 and 7. The VSR can be related to the crosslink density (75). The swelling data are plotted in Fig. 9 as 1-Z, where Z is the change in VSR between coal and char normalized by the maximum change. For coal, Z is 0 and for completely crosslinked char, Z is one. The weight loss profiles in Figs. 6a and 7a of the two samples look similar, but the swelling behaviors in Fig. 9 are quite different. The Pittsburgh Seam coal starts to crosslink during tar evolution and the Beulah lignite crosslinks well before tar evolution. Similar results have been reported by Suuberg et al. (57) who also suggested a correlation between crosslinking in lignites and CO_2 evolution. The coals which undergo early crosslinking are less fluid, produce less tar and produce lower molecular weight tar compared with coals which don't experience early crosslinking (30,31,44).

As discussed previously, under the assumption that the crosslinking reactions may also release gas species, the VSR was correlated with the observed evolution of gas species during pyrolysis. Correlations presented in Fig. 2 show that on a molar basis, the evolution of CO_2 from the lignite and CH_4 from the bituminous coal appear to have similar effects on the VSR. Reactions which form these gases, leave behind free radicals which can be stabilized by crosslinking.

Assuming that one crosslink is formed for each CO_2 or CH_4 evolved from the char, the FG-DVC model predictions are presented as the lines in Figs. 2 and 9.

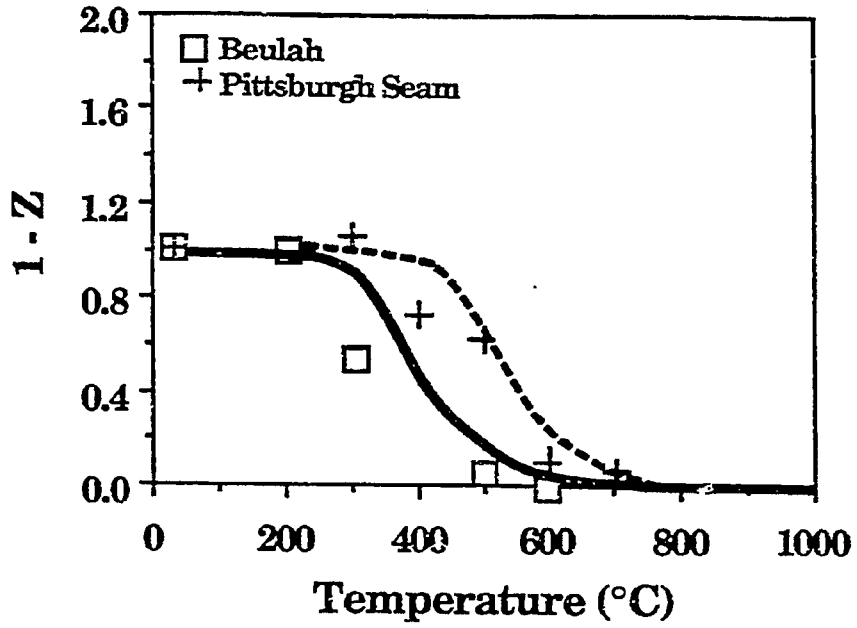

Figure 9. Comparison of Measured and Predicted Normalized Volumetric Swelling Ratio as a Function of Temperature. Heating Rate is 0.5°C/sec in N_2 . Solid Line is Prediction for Beulah Lignite, Dashed Line for Pittsburgh Seam Coal.

The agreement between theory and experiment is good except for the following: in Fig. 9, the increase in VSR, presumably due to bond breaking, has not been included in the model; in Fig. 2 the loss in VSR (increase in Z) is overpredicted for the Pittsburgh Seam coal for the same reason.

The difference in crosslinking behaviors are manifested in several areas. At low heating rates, the Pittsburgh Seam chars soften, the Beulah chars do not. This is in agreement with the high predicted maximum extract yields in the Pittsburgh char 69.5% compared to the low yields in the Zap lignite 6.8%. The measured values are 70.9% (Ref. 16) and ~6%, respectively. The predicted yields of tar plus aliphatic gases at 1 atmosphere, 0.5°C/sec to 900°C, of 26.2% and 11.1% are in good agreement with measured values of 28.1% and 6.0% for the Pittsburgh and Beulah, respectively.

Molecular Weight Distribution

A sensitive test of the general model is the ability to predict tar molecular weight distributions. These have been shown to vary systematically with rank (30,31). Figures 10c and 10d show results for the Pittsburgh Seam bituminous and the Beulah lignite pyrolyzed in the FIMS apparatus. The data have been summed over 50 amu intervals. While the Pittsburgh bituminous shows a peak intensity at about 400 amu, the lignite peak is at 100 amu. The predicted average tar molecular weight distributions are in good agreement with FIMS data as shown in Fig. 10a and 10b. The enhanced drop off in amplitude with increased molecular weight for the lignite compared to the bituminous coal is due to early crosslinking in the lignite.

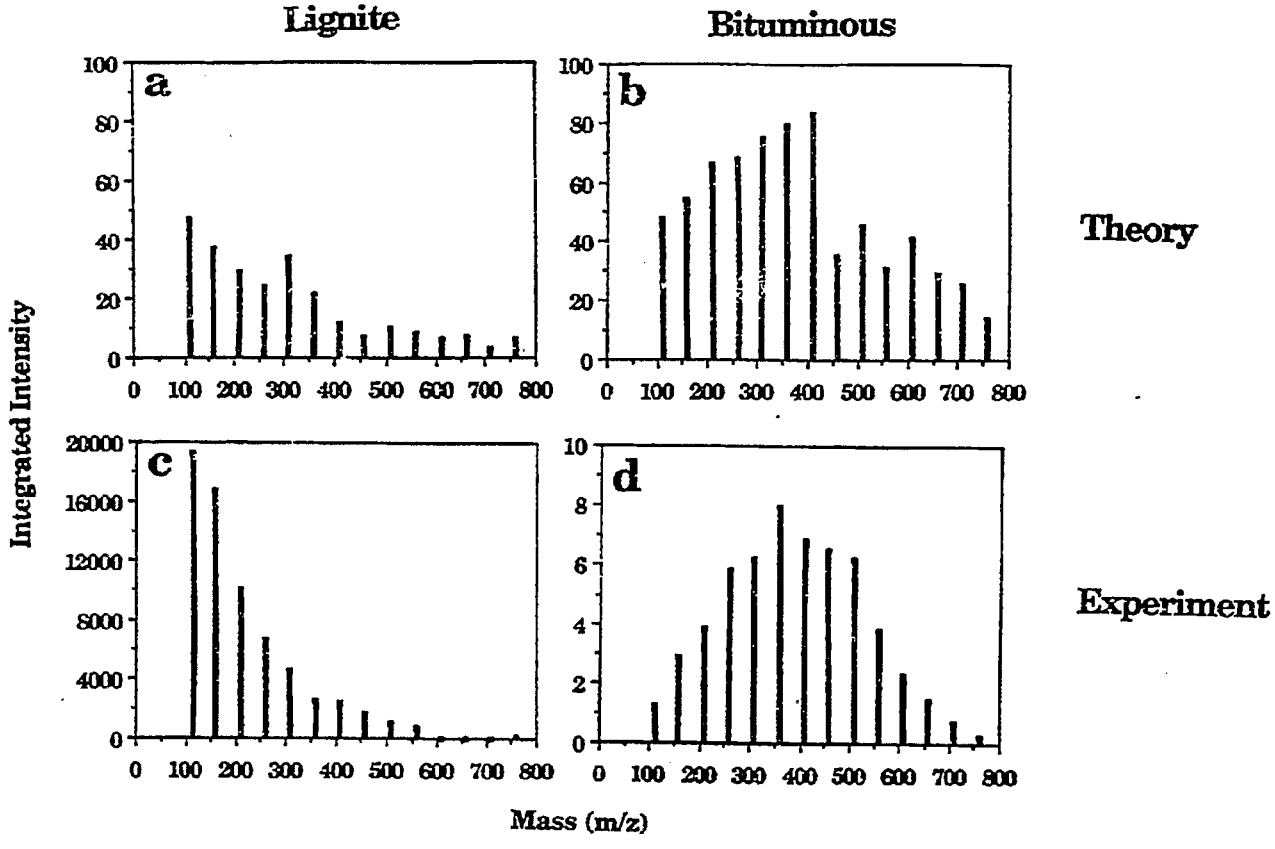

Figure 10. Comparison of Measured and Predicted Tar Molecular Weight Distributions for Lignite and Bituminous Coals. The Experiments are Performed by Pyrolysis of Coal Samples in a FIMS Apparatus. Intensities have been Summed Over 50 amu Intervals.

Pressure Effects

The predicted effect of pressure on the tar molecular weight distribution is illustrated in Figs. 11a and 11b. Pressure enters the model through the transport Eqs. 3 and 4. The internal transport rate (Eq. 4) is inversely proportional to the ambient pressure P_o and the diffusivity D_j in Eq. 3 is reduced with increasing pressure. The reduced transport rate reduces the evolution of the heavier molecules. Therefore, the average molecular weight and the vaporization "cut-off" decrease with increasing pressure. The trends are in agreement with observed tar molecular weight distributions shown in Figs. 11c and 11d. The spectra are for previously formed tar which has been collected and analyzed in a FIMS apparatus (58). The low values of intensity between 100 and 200 mass units may be due to loss of these components in collection and handling due to their higher volatility.

Pressure effects on yields have also been examined. Figure 12 compares the predicted and measured pressure dependence on yield for a Pittsburgh Seam coal. Figure 12a compares to the total volatile yield data of Anthony et al. (22) while Fig. 12b compares to the tar plus liquids data of Suuberg et al. (7). The agreement between theory and experiment is good at one atmosphere and above, but the theory with $\Delta P = 0$ (solid line) overpredicts the yields at low pressure. Below one atmosphere, it is expected that ΔP within the particle will become important compared to the ambient pressure, P_o. The dashed line, which agrees with the data were obtained assuming $\Delta P = 0.2$ atm which is physically reasonable.

Heating Rate Effects

It has been found that Beulah lignite chars soften and exhibit bubble formation at high heating rates ($\sim$20,000°C/s) (13). Under these conditions,

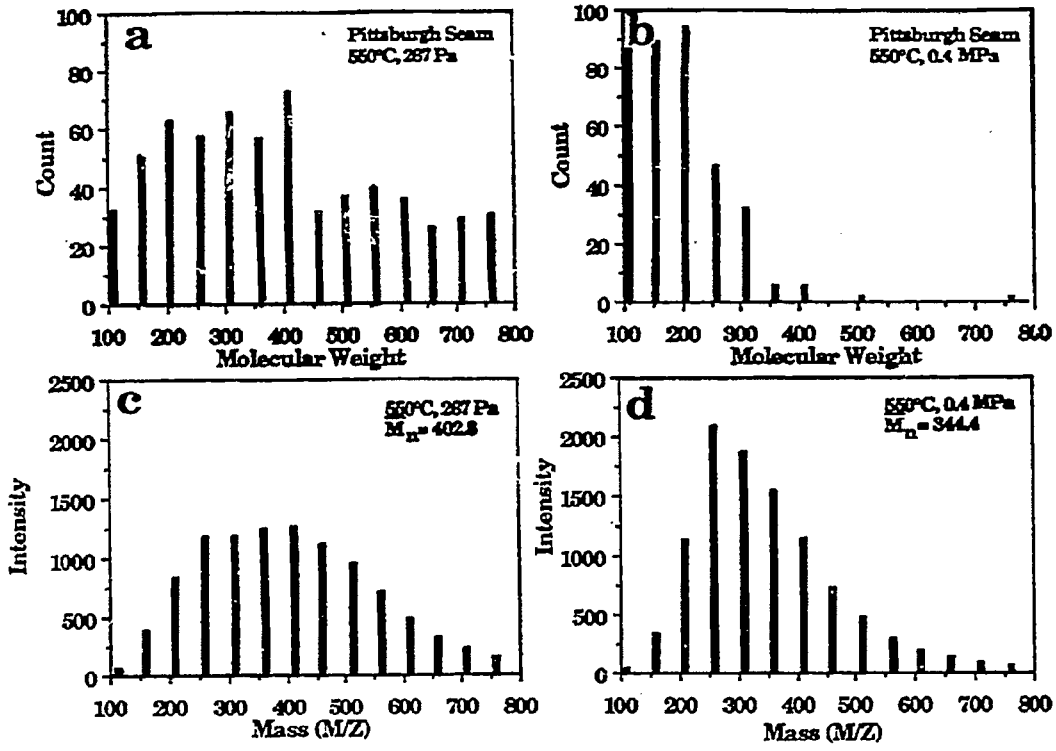

Figure 11. Comparison of Predicted (a and b) and Measured (c and d) Tar Molecular Weight Distribution for Pyrolysis of a Pittsburgh Seam Coal in a Heated Grid Apparatus at a Heating Rate of 500°C/sec to 550°C. Figure a and c Compare the Prediction and the Measurement at 267 Pa. Figure b and d Compare the Prediction and Measurement at 0.4 MPa.

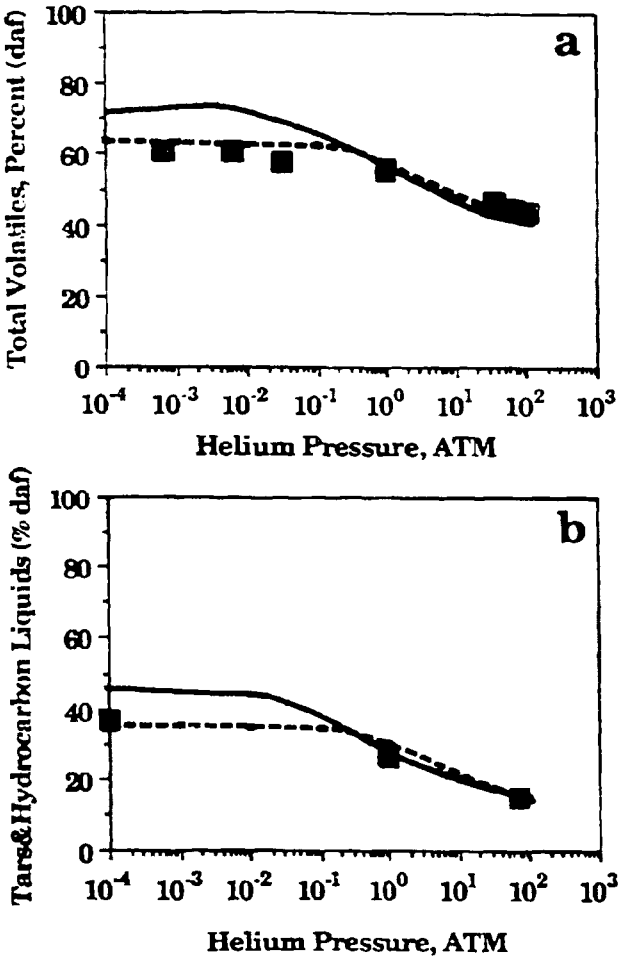

Figure 12. Comparison of Measured and Predicted Volatile Yields with Pressure. a) Total Volatile; Data of Anthony et al. (22). b) Tars and Hydrocarbon Liquids; Data of Suuberg et al. (7). Solid Line Assume $\Delta P = 0$, Dashed Line Assume $\Delta P = 0.2$ ATM.

molecular weight distribution of tars of Beulah lignite look like that of a bituminous coal (30,31). The infrared spectrum of the tar is also closer in appearance to that of the parent coal (31). The mass spectra of the tars formed at low heating rate (0.05°C/s) and high heating rate (20,000°C/s) are shown in Figs. 13a and 13b, respectively. The low values of intensity between 100 and 200 mass units in Fig. 13b is beleived to be due to loss of these components in collection and handling due to their high volatility. The molecular weight distribution of the tars is very sensitive to the heating rate. The effect is attributed to the higher rate of depolymerization reactions relative to crosslinking reactions at high temperatures.

The model including the internal transport was used to simulate the low heating rate (0.05°C/s) and high heating rate (20,000°C/s) pyrolysis of Beulah lignite. The activation energy for CO_2 (extra loose) in the FG subroutine was reduced from 60 kcal/mole to 45 kcal/mole in order to make it lower than the activation energy for bond breaking (55 kcal/mole). This change in the activation energy makes only a slight change in the CO_2 evolution profiles for high heating rate (20,000°C/s) and low heating profiles (0.5°C/s). The CO_2 gas evolution profiles are compared to the data in Figs. 14a and 14b for high heating rate (20,000°C/s) and low heating rate (0.5°C/s) for Beulah lignite using activation energies of 55,45 and 30 kcal/mole.. When the activation energy for CO_2 (extra loose) was reduced to 30 kcal/mole, the high heating rate CO_2 evolution profile was quite different and did not agree with the experimental data.

The model with internal transport and the altered activation energy for CO_2 (extra loose) evolution was used to simulate the tar molecular weight distributions with $P = 0$ atm for Beulah lignite for high heating rate (20,000°C/s) and low heating rate (0.05°C/s) in Figs. 15a and 15b, respectively. The tar molecular

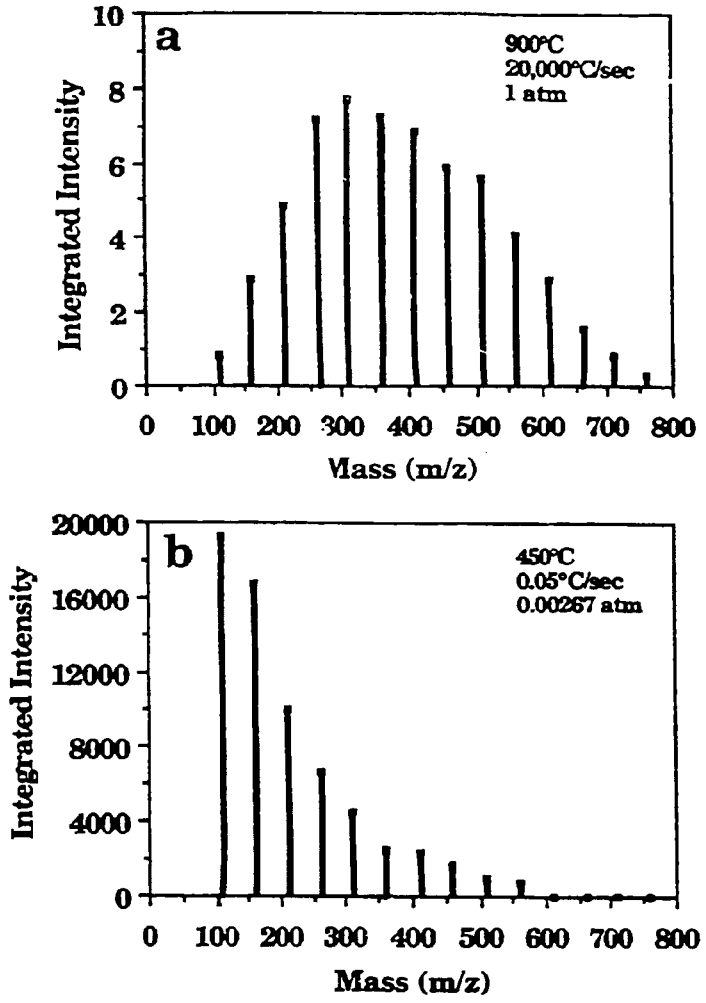

Figure 13. Comparison of FIMS Spectra of Tars of Zap Lignite Formed at a) High Heating Rate (20,000°C/sec) and b) Low Heating Rate (0.05°C/sec).

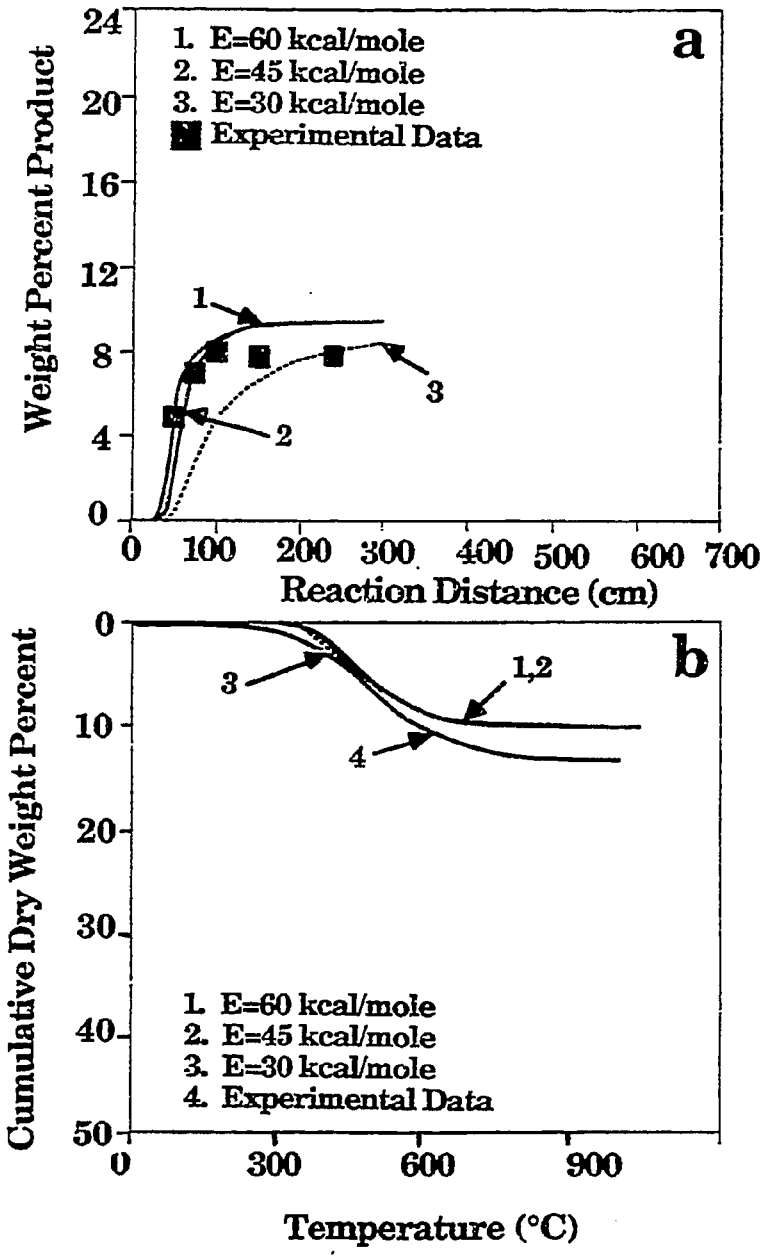

Figure 14. Comparison of CO_2 Evolution at Low Heating Rate (0.5°C/sec) and High Heating Rate (20,000°C/sec) with Model Predictions for Different Values of Activation Energy for CO_2 (extra loose) in the FG-DVC Model.

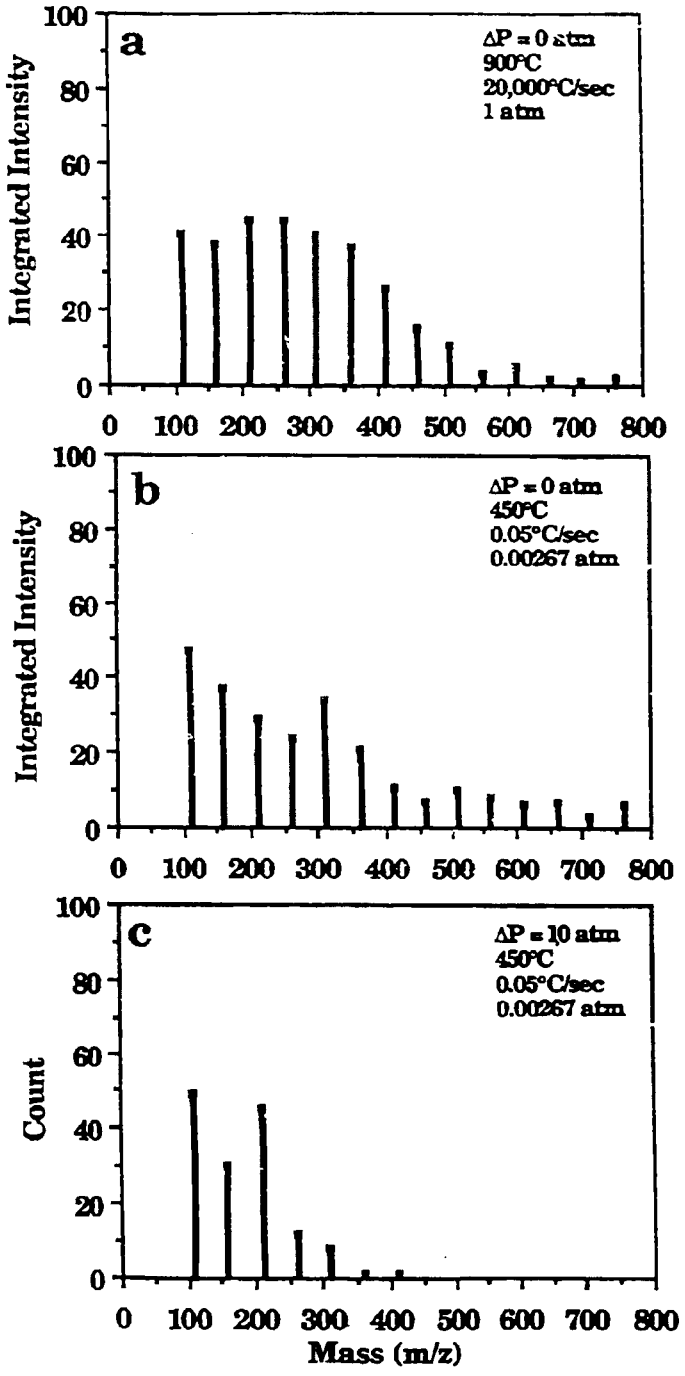

Figure 15. Comparison of Predicted Molecular Weight Distribution of Tars of Beulah Lignite for a) High Heating Rate (20,000°C/sec), $\Delta P = 0$; and b) and c) Low Heating Rate (0.05°C/sec). In b) $\Delta P = 0$, in c) $\Delta P = 10$ atm.

weight distributions (for ΔP = 0 atm) at high and low heating rates show the observed trend of the tar molecular weight distribution on heating rate. At high heating rate, where crosslinking reactions are curbed and the lignite melts, ΔP is likely to be low. At low heating rate, due to the higher extent of crosslinking before tar evolution, the coal is less fluid and hence, ΔP (which is related to viscosity of the solid/liquid mixture) is likely to be higher. A simulation for ΔP = 10 atm is shown in Fig. 15c. The observed molecular weight distribution in Fig. 13b appears to be intermediate between the ΔP = 0 and ΔP = 10 atm cases.

CONCLUSIONS

A general FG-DVC model for coal devolatilization which combines a functional group model for gas evolution and a statistical model for tar formation has been presented. The tar formation model includes depolymerization, crosslinking, external transport and internal transport. The crosslinking is related to the formations of CO_2 and CH_4 species evolution, with one crosslink formed per molecule evolved. The predictions of the tar formation model are made using Monte Carlo methods.

The FG-DVC model predictions compare favorably with a variety of data for the devolatilization of Pittsburgh Seam coal and North Dakota (Beulah) lignite, including volatile yields, extract yields, crosslink densities and tar molecular weight distributions. The variations with pressure, devolatilization temperature, rank and heating rate were accurately predicted. While film diffusion appears to limit surface evaporation and the transport of tar when devolatilization occurs at high temperatures, internal transport appears to dominate when devolatilization occurs at low temperatures.

The rank dependence of tar formation, extract yields, crosslinking, and viscosity appears to be explained by the rank dependence of CO_2 yields. High CO_2 yields in low rank coals produces rapid crosslinking at low temperatures and hence low tar yields, low extract yields, loss of solvent swelling properties and high viscosities. The relative importance of crosslinking compared to bond breaking is, however, sensitive to heating rate and this effect is predicted by the FG-DVC model.

ACKNOWLEDGMENT

This work was supported under DOE Contracts DEAC21-85MC22050, DEAC21-84MC21004, DE-AC21-86MC23075 and DE-FG22-85PC80910. The authors wish to express their thanks to Professor Eric Suuberg for many helpful discussions on transport properties.

REFERENCES

1. Howard, J.B., Peters, W.A., and Serio, M.A., "Coal Devolatilization Information for Reactor Modeling", Final Report EPRI Project No. 986-5, (1981).
2. Howard, J.B., Chemistry of Coal Utilization, (M.A. Elliott, Ed.), John Wiley, NY, Chapter 12, p 665, (1981).
3. Gavalas, G.R., Coal Pyrolysis, Elsevier Sci., Amsterdam, The Netherlands, (1982).
4. Suuberg, E.M., in Chemistry of Coal Conversion, (R.H. Schlosberg, Ed.), Chapter 4, Plenum Press, NY (1985).
5. Solomon, P.R. and Hamblen, D.G., in Chemistry of Coal Conversion, (R.H. Schlosberg, Editor), Plenum Press, NY, Chapter 5, pg. 121, (1985).
6. Serio, M.A., Hamblen, D.G., Markham, J.R., and Solomon, P.R., Energy and Fuels, **1**, (2), 138, (1987).
7. Suuberg, E.M., Peters, W.A., and Howard, J.B., 17th Symp. (Int) on Combustion, The Combustion Institute, Pittsburgh, PA, pg. 117, (1979).
8. Juntgen, H. and van Heek, K.H., Fuel Processing Technology, **2**, 261, (1979).
9. Weimer, R.F. and Ngan, D.Y., ACS Div. of Fuel Chem. Preprints, **24**, #3, 129, (1979).
10. Campbell, J.H., Fuel, **57**, 217, (1978).
11. Solomon, P.R. and Colket, M.B., 17th Symposium (Int) on Combustion; The Combustion Institute, Pittsburgh, PA, 131, (1979).
12. Solomon, P.R., Hamblen, D.G., Carangelo, R.M., and Krause, J.L., 19th Symposium (Int) on Combustion, The Combustion Institute, Pittsburgh, PA, 1139, (1982).
13. Solomon, P.R., Serio, M.A., Carangelo, R.M., and Markham, J.R., Fuel, **65**, 182, (1986).
14. Xu, W.-C., and Tomita, A., Fuel, **66**, 627, (1987).
15. Juntgen, H., Fuel, **63**, 731, (1984).
16. Fong, W.S., Peters, W.A., and Howard, J.B., Fuel, **65**, 251, (1986).
17. Oh, M., Peters, W.A., and Howard, J.B., Proc. of the 1983 Int. Conf. on Coal Sci., p 483, International Energy Agency, (1983).
18. Fong, W.S., Khalil, Y.F., Peters, W.A. and Howard, J.B., Fuel, **65**, 195 (1986).
19. van Krevelen, D.W., Properties of Polymers, Elsevier, Amsterdam (1976).
20. Solomon, P.R., New Approaches in Coal Chemistry, ACS Symposium Series **169**, American Chemical Society, Washington, DC, pp 61-71, (1981).
21. van Krevelen, D.W. and Schuyer, J., Coal Science, Elsevier, Amsterdam, (1957).
22. Anthony, D.B., Howard, J.B., Hottel, H.C., and Meissner, H.P., 15th Symp. (Int) on Combustion, The Combustion Institute, Pittsburgh, PA, pg. 1303, (1974).
23. Unger, P.E. and Suuberg, E.M., 18th Symp. (Int) on Combustion, The Combustion Institute, Pittsburgh, PA, pg. 1203, (1981).
24. Russel, W.B., Saville, D.A., and Greene, M.I., AIChE J., **25**, 65, (1979).
25. James, R.K. and Mills, A.F., Letters in Heat and Mass Transfer, **3**, 1, (1976).
26. Lewellen, P.C., S.M. Thesis, Department of Chemical Engineering, MIT, (1975).
27. Chen, L.W. and Wen, C.Y., ACS Div. of Fuel Chem. Preprints, **24**, (3), p141, (1979).
28. Niksa, S. and Kerstein, A.R., Combustion and Flame, **66**, (2), 95, (1986).
29. Niksa, S. Combustion and Flame, **66**, #2, 111, (1986).
30. Solomon, P.R., Squire, K.R., Carangelo, R.M., proceedings of the International Conference on Coal Science, Sydney, Australia, pg. 945, (1985).
31. Solomon, P.R. and Squire, K.R., ACS Div. of Fuel Chem. Preprints, **30**, #4, 347, (1985).

32. Suuberg, E.M., Unger, P.E., and Lilly, W.D., Fuel, **64**, 956, (1985).
33. Solomon, P.R., Hamblen, D.G., Carangelo, R.M., Serio, M.A., and Deshpande, G.V., ACS Div. of Fuel Chem. Preprints, **32**, #3, 83, (1987).
34. Gavalas, G.R. and Wilks, K.A., AIChE, **26**, 201, (1980).
35. Simons, G.A., Prog. Energy Combust. Sci., **9**, 269, (1983).
36. Suuberg, E.M. and Sezen, Y., Proc. of the 1985 Int. Conf. on Coal Sci., p 913, Pergamon Press, (1985).
37. Melia, P.F. and Bowman, C.T., Combust. Sci. Technol. **31**, 195 (1983); also An analytical model for coal particle pyrolysis and swelling, paper presented at the Western States Section of the Combustion Institute, Salt Lake City, 1982.
38. Kobayashi, H., Howard, J.B., and Sarofim, A.F., 16th Symposium (Int) on Combustion, The Combustion Institute, Pittsburgh, PA, pg. 411, (1977). and Kobayashi, H., Ph.D. Thesis, MIT Dept. of Mechanical Eng., Cambridge, MA, (1976).
39. Niksa, S., Heyd L.E., Russel, W.B., and Saville, D.A., 20th Symposium (Int) on Combustion, The Combustion Institute, Pittsburgh, PA, pg 1445, (1984).
40. Badzioch, S. and Hawksley, P.G.W., Ind. Eng. Chem. Proc. Des. Dev., **9**, 521, (1970).
41. Freihaut, J.D., Ph.D. Thesis, Pennsylvania State University, (1980).
42. Maloney, D.J. and Jenkins, R.G., 20th Symposium (Int) on Combustion, The Combustion Institute, Pittsburgh, PA, pg. 1435, (1984).
43. Witte, A.B. and Gat, N., "Effect of Rapid Heating on Coal Nitrogen and Sulfur Release", presented at the DOE Direct Utilization AR&TD Contractor's Meeting, Pittsburgh, PA, (1983).
44. Solomon, P.R. and King, H.H., Fuel, **63**, 1302, (1984).
45. Solomon, P.R., Squire, K.R., and Carangelo, R.M., ACS Div. of Fuel Chem. Preprints, **29**, (1), 10, (1984).
46. Squire, K.R., Solomon, P.R., Carangelo, R.M., and DiTaranto, M.B., Fuel, **65**, 833, (1986).
47. Squire, K.R., Solomon, P.R., DiTaranto, M.B., and Carangelo, R.M., ACS Div. of Fuel Chem. Preprints, **30**, #1, 386, (1985).
48. Gavalas, G.R., Cheong, P.H., and Jain, R., Ind. Eng. Chem. Fundam. **20**, 113, (1981).
49. Gavalas, G.R., Cheong, P.H., and Jain, R., Ind. Eng. Chem. Fundam. **20**, 122, (1981).
50. Solomon, P.R. and Hamblen, D.G., Prog. Energy Combust. Sci., **9**, 323, (1983).
51. Xu, W.C. and Tomita, A., Fuel, **66**, 632, (1987).
52. Agarwal, P.K., Fuel, **64**, 870, (1985).
53. Agrwal, P.K., Agnew, J.B., Ravindran, N. and Weimann, R., Fuel, **66**, 1097, (1987).
54. Vorres, K.S., ACS Div. of Fuel Chem. Preprints, **32**, (4), 221, (1987).
55. Green, T.K., Kovac, J., and Larsen, J.W., Fuel, **63**, #7, 935, (1984).
56. Green, T.K., Kovac, J., and Larsen, J.W., in Coal Structure, (R.A. Meyers, Editor), Academic Press, NY, (1982).
57. Suuberg, E.M., Lee, D., and Larsen, J.W., Fuel, **64**, 1668, (1985).
58. St. John, G.A., Butrill, Jr., S.E. and Anbar, M., ACS Symposium Series, **71**, p. 223 (1978).
59. Carangelo, R.M., Solomon, P.R. and Gerson, D.J., Fuel, **66**, 960, (1987).
60. Solomon, P.R. and Colket, M.B., Fuel, **57**, 748, (1978).
61. Brown, J.K., Dryden, I.G.C., Dunevein, D.H., Joy, W.K., and Pankhurst, K.S., J. Inst. Fuels, **31**, 259, (1958).
62. Orning, A.A. and Greifer, B., Fuel, **35**, 318, (1956).

63. Solomon, P.R., Hamblen, D.G., Carangelo, R.M., Serio, M.A., and Deshpande, G.V., "Models of Tar Formation During Coal Devolatilization", Combustion and Flame, (1987), to be published.
64. Nelson, P.F., Fuel, **66**, 1264, (1987).
65. Calkins, W.H., Hagaman, E., and Zeldes, H., Fuel, **63**, 1113, (1984).
66. Calkins, W.H. and Tyler, R.J., Fuel, **63**, 1119, (1984).
67. Calkins, W.H., Fuel, **63**, 1125, (1985).
68. Calkins, W.H., Hovsepian, B.K., Drykacz, G.R., Bloomquist, C.A.A., and Ruscic, L., Fuel, **63**, 1226, (1984).
69. Solomon, P.R., Coal Structure, ACS Advances in Chemistry Series, **192**, 7, Washington, DC, (1981).
70. Freihaut, J.D., Proscia, W.M., and Seery, D.J., "Effect of Heat Transfer on Tar and Light Gases from Coal Pyrolysis", presented at the 194th National Meeting of the American Chemical Society, New Orleans, LA, (Aug. 31 - Sept. 4, 1987).
71. Stein, S.E., New Approaches in Coal Chemistry, (B.D. Blaustein, B.C. Bockrath, and S. Friedman, Editors), ACS Symposium Series, **169**, 208, Am. Chem. Soc. Washington, DC, (1981).
72. Stein, S.E., "Multistep Bond Breaking and Making Processes of Relevance to Thermal Coal Chemistry", Annual Report for GRI Contract No. 5081-261-0556. Accession No. GRI-81/0147, (1983).
73. Stein, S.E., Robaugh, D.A., Alfieri, A.D., and Miller, R.E., "Bond Homolysis in High Temperature Fluids", Journal of Amer. Chem. Society, **104**, 6567, (1982).
74. Solomon, P.R., Hamblen, D.G., Deshpande, G.V. and Serio, M.A., A General Model of Coal Devolatilization, International Coal Science Conference, The Netherlands, October 1987.
75. Nelson, J.R., Fuel, **62**, 112, (1983).
76. Pitt, G.J., Fuel, **41**, 267, (1962).
77. Rennhack, "Zur Kinetik der Entgasung von Schwelkoks," Brennstoff-Chemie, **45**, 300 (1964).
78. Hanbaba, P., Juntgen, H. and Peters, W., "Nicht-isotherme Reaktionskinetik der Kohlenpyrolyse, Teil II. Erweiterung der Theorie der Gasabspaltung und experimentelle Bestatigung an Steinkohlen," Brennstoff-Chemie,**49**, 368 (1968).
79. Van Heek, K.H., Juntgen, H. and Peters, W., "Kinetik nicht-isotherm ablaufender Reaktionen am Beispiel," Ber. Busenges, Phys. Chem, **71**, 113 (1967).

U.S. DEPARTMENT OF COMMERCE
Technology Administration
National Technical Information Service
Springfield, VA 22161 (703) 605-6000